Impacts of Model Top Altitude on Satellite Data Assimilation for Hurricane Forecasts

Xiaolei Zou

Department of Earth, Ocean and Atmospheric Science

Florida State University

December 18, 2013

Outline

- **A Brief Overview of 3D-Var**
  - ✓ Mathematical Formulation
  - ✓ Theoretical Basis
- **Quality Control of Satellite Data**
  - ✓ Comparison between AMSU and ATMS
  - ✓ Advantage of ATMS for Cloud Detection
- **Impact of Satellite Data Assimilation on TC Forecasts**
  - ✓ Impact of Model Top Altitude
  - ✓ Impact of ATMS Radiance Assimilation
- **Summary, Current and Future Plan**

Three-Dimensional Variational (3D-Var) Data Assimilation

$$J(\mathbf{x}) = \frac{1}{2}(\mathbf{x}-\mathbf{x}_b)^T \mathbf{B}^{-1}(\mathbf{x}-\mathbf{x}_b) + \frac{1}{2}(H(\mathbf{x})-\mathbf{y}^{obs})^T(\mathbf{O}+\mathbf{F})^{-1}(H(\mathbf{x})-\mathbf{y}^{obs})$$

$$J(\mathbf{x}_a) = \min_{\mathbf{x}} J(\mathbf{x}) \quad \forall \mathbf{x} \text{ near } \mathbf{x}_b$$

- $\mathbf{x}$ – analysis variable
- $\mathbf{x}_a$ – final analysis
- $\mathbf{x}_b$ – background
- $\mathbf{B}$ – background error covariance
- $\mathbf{y}^{obs}$ – observations
- $\mathbf{O}$ – observation error covariance
- H – observation operator
- $\mathbf{F}$ – forward model error covariance

- NCEP GSI 3D-Var Data Assimilation System
- Hurricane Weather Research Forecast (HWRF) Model

A Statistical Derivation of the 3D-Var Formulation

The probability distribution functions of three sources of information (Tarantola, 1987):

$$\begin{aligned} &\mathbf{y}^{obs} && - p_{obs}(\mathbf{y}|\mathbf{y}^{obs}) \\ &\mathbf{x}_b && - p_b(\mathbf{x}|\mathbf{x}_b) \\ &H(\mathbf{x}) && - p_H(\mathbf{y}|H(\mathbf{x})) \end{aligned}$$

The PDF of the *a posteriori* state of information is

$$\sigma(\mathbf{x},\mathbf{y}) = p_b p_{obs} p_H$$

The PDF of the *a posteriori* state of information in model space is

$$\sigma(\mathbf{x}) = \int \sigma(\mathbf{x},\mathbf{y})d\mathbf{y} = p_b(\mathbf{x}\,|\,\mathbf{x}^b)\int p_{obs}(\mathbf{y}\,|\,\mathbf{y}^{obs})p_H(\mathbf{y}\,|\,H(\mathbf{x}))d\mathbf{y}$$

A Statistical Derivation of the 3D-Var Formulation

Assuming all errors are unbiased and Gaussian:

$$p_{obs}(\mathbf{y}|\mathbf{y}^{obs}) = C_1 \exp\left(-\frac{1}{2}\left(\mathbf{y}-\mathbf{y}^{obs}\right)^T \mathbf{O}^{-1}\left(\mathbf{y}-\mathbf{y}^{obs}\right)\right)$$

$$p_b(\mathbf{x}|\mathbf{x}_b) = C_2 \exp\left(-\frac{1}{2}\left(\mathbf{x}-\mathbf{x}_b\right)^T \mathbf{B}^{-1}\left(\mathbf{x}-\mathbf{x}_b\right)\right)$$

$$p_H(\mathbf{y}|H(\mathbf{x})) = C_3 \exp\left(-\frac{1}{2}\left(\mathbf{y}-H(\mathbf{x})\right)^T \mathbf{F}^{-1}\left(\mathbf{y}-H(\mathbf{x})\right)\right)$$

The PDF of the *a posteriori* state of information in model space is

$$\sigma(\mathbf{x}_0) = p_b(\mathbf{x}_0 \,|\, \mathbf{x}^b)\int p_{obs}(\mathbf{y}\,|\,\mathbf{y}^{obs})p_H(\mathbf{y}\,|\,H(\mathbf{x}_0))d\mathbf{y}$$

⇓ simply becomes

$$\sigma(\mathbf{x}) = C\exp\left\{-\left[\frac{1}{2}(\mathbf{x}-\mathbf{x}_b)^T\mathbf{B}^{-1}(\mathbf{x}-\mathbf{x}_b)+\frac{1}{2}(H(\mathbf{x})-\mathbf{y}^{obs})^T(\mathbf{O}+\mathbf{F})^{-1}(H(\mathbf{x})-\mathbf{y}^{obs})\right]\right\}$$

A Statistical Derivation of the 3D-Var Formulation

The PDF of the *a posteriori* state of information in model space

$$\sigma(\mathbf{x}) = C\exp\left\{-\left[\frac{1}{2}(\mathbf{x}-\mathbf{x}_b)^T\mathbf{B}^{-1}(\mathbf{x}-\mathbf{x}_b)+\frac{1}{2}(H(\mathbf{x})-\mathbf{y}^{obs})^T(\mathbf{O}+\mathbf{F})^{-1}(H(\mathbf{x})-\mathbf{y}^{obs})\right]\right\}$$

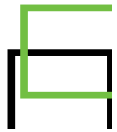

$$\sigma(\mathbf{x}) = Ce^{-J(\mathbf{x})}$$

Conclusion:

The minimum of $J(\mathbf{x})$, which is obtained by the 3D-Var, is the maximum likelihood estimate of the *a posteriori* state of information in the model space $\sigma(\mathbf{x})$!

Suomi NPP Satellite

Six Instruments

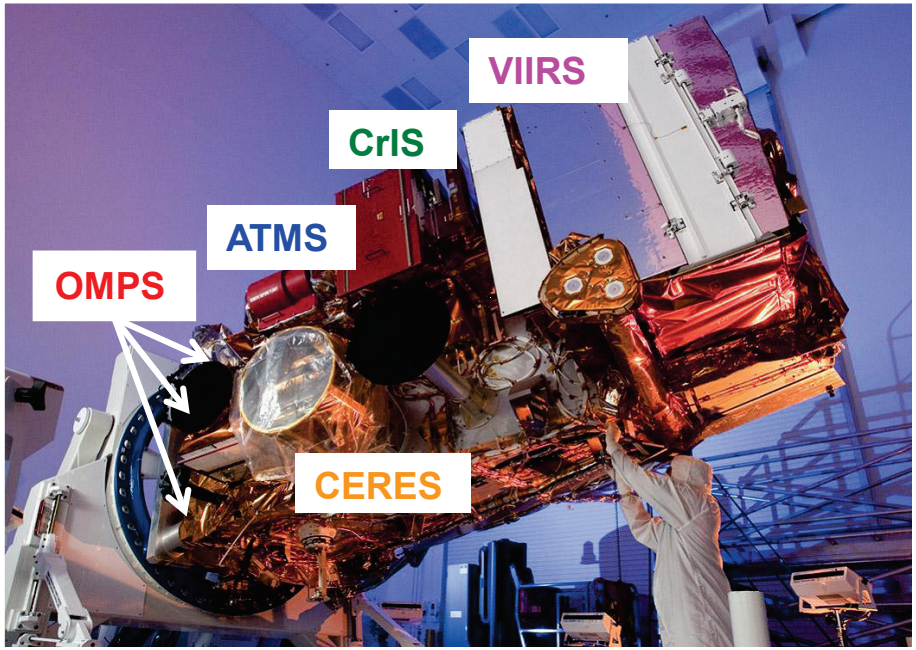

ATMS --- Advanced Technology Microwave Sounder

CrIS --- Cross-track Infrared Sounder

VIIRS --- Visible/Infrared Imager/Radiometer Suite

OMPS --- Ozone Mapping and Profiler Suite

CERES --- Cloud and Earth Radiant Energy System

Channel Characteristics of ATMS and AMSU

Channel		Frequency (GHz)		NEΔT (K)		Beam width (°)		Peak WF (hPa)	
ATMS	AMSU	ATMS	AMSU	ATMS	AMSU	ATMS	AMSU	ATMS	AMSU
1		23.8		0.50	0.30	5.2	3.3	Surface	
2		31.4	31.399	0.60	0.30	5.2	3.3	Surface	
3		50.3	50.299	0.70	0.40	2.2	3.3	Surface	
4		51.76		0.50		2.2		Surface	
5	4	52.8		0.50	0.25	2.2	3.3	1000	
6	5	53.596±0.115		0.50	0.25	2.2	3.3	700	
7	6	54.4		0.50	0.25	2.2	3.3	400	
8	7	54.94		0.50	0.25	2.2	3.3	270	
9	8	55.5		0.50	0.25	2.2	3.3	180	
10	9	57.29		0.75	0.25	2.2	3.3	90	
11	10	57.29± 0.217		1.00	0.40	2.2	3.3	50	
12	11	57.29± 0.322± 0.048		1.00	0.40	2.2	3.3	25	
13	12	57.29± 0.322 ± 0.022		1.25	0.60	2.2	3.3	12	
14	13	57.29± 0.322 ± 0.010		2.20	0.80	2.2	3.3	5	
15	14	57.29± 0.322± 0.0045		3.60	1.20	2.2	3.3	2	
16	15	88.2	89.0	0.30	0.50	2.2	3.3	Surface	
17	16	165.5	89.0	0.60	0.84	1.1	1.1	1000	Surface
18	17	183.31±7.0	157.0	0.80	0.84	1.1	1.1	800	Surface
19	18	183.31±4.5	183.31±1.0	0.80	0.60	1.1	1.1	700	400
20	19	183.31±3.0		0.80	0.70	1.1	1.1	600	
21	20	183.31±1.8	183.31±7.0	0.80	1.06	1.1	1.1	500	800
22		183.31±1.0		0.90		1.1		400	

ATMS

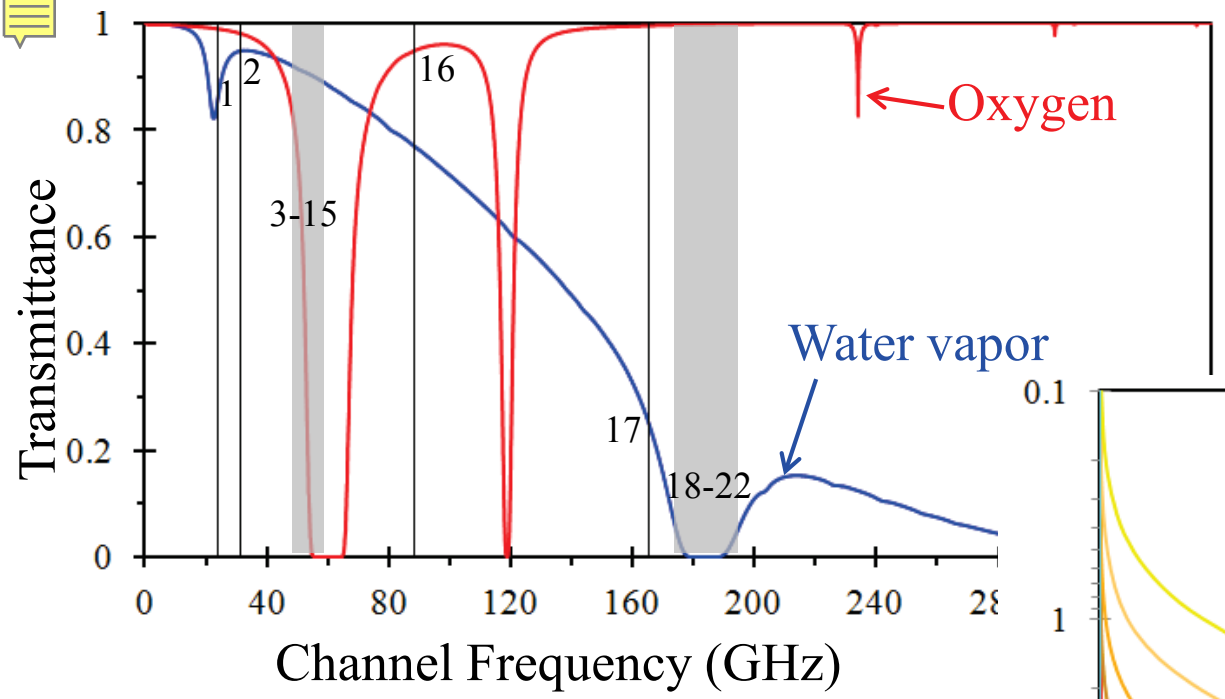

ATMS Channels 1-16:

23.8 – 88.2 GHz

ATMS Channels 17-22:

165.5 – 183.31 ± 7.0 GHz

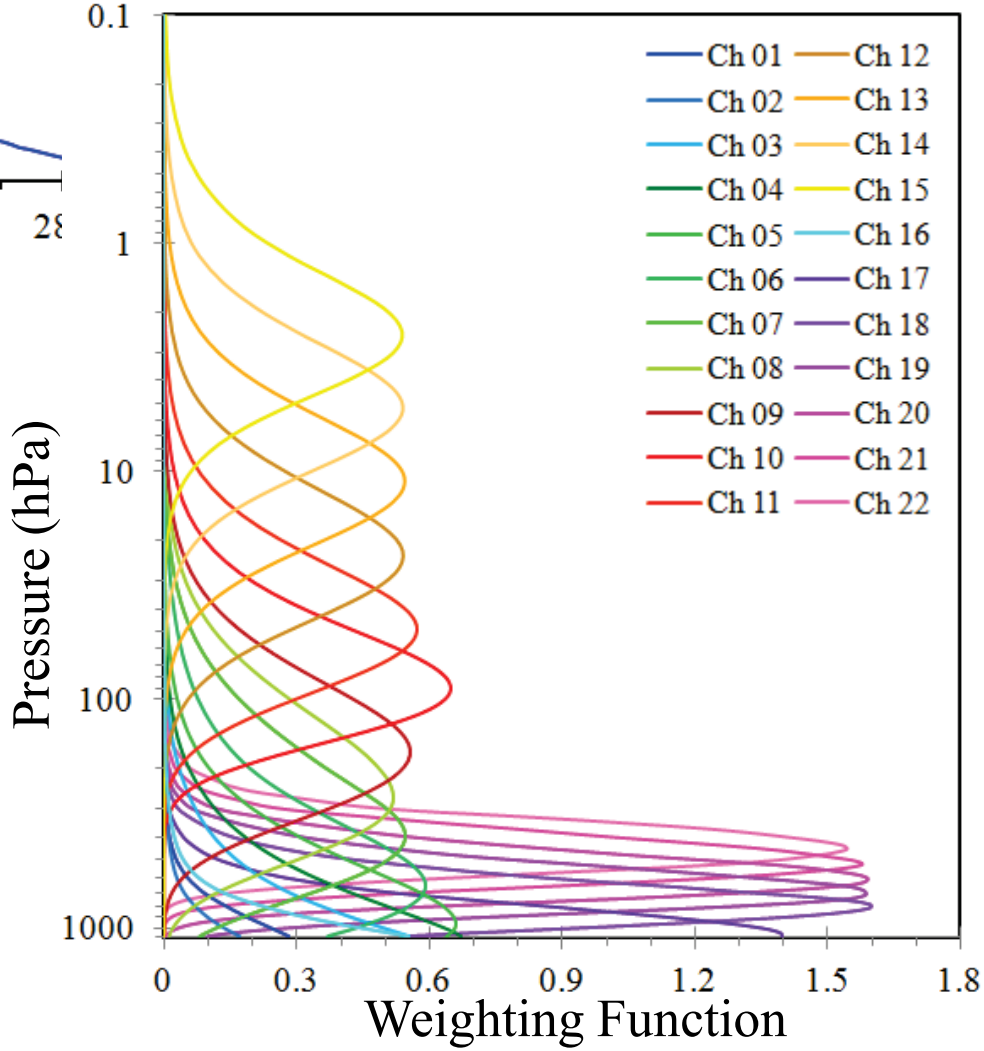

Cloud Liquid Water Path (LWP) Retrieval Using Two AMSU-A Window Channels

$$L = a_0 \cos\theta \left(\ln(T_s - T_{b31}) - a_1 \ln(T_s - T_{b23}) - a_2 \right)$$

θ – satellite zenith angle

T_s – surface temperature

$T_{b,23}$ – brightness temperature at 23.8 GHz

$T_{b,31}$ – brightness temperature at 31.4 GHz

Weng, F., L. Zhao, R. R. Ferraro, G. Poe, S. Li, and N. C. Grody, 2003: Advanced microwave sounding unit cloud and precipitation algorithms, *Radio Sci.*, 3**8**(4), 80-86.

FOV Comparison between ATMS and AMSU-A for Window Channels 1-2

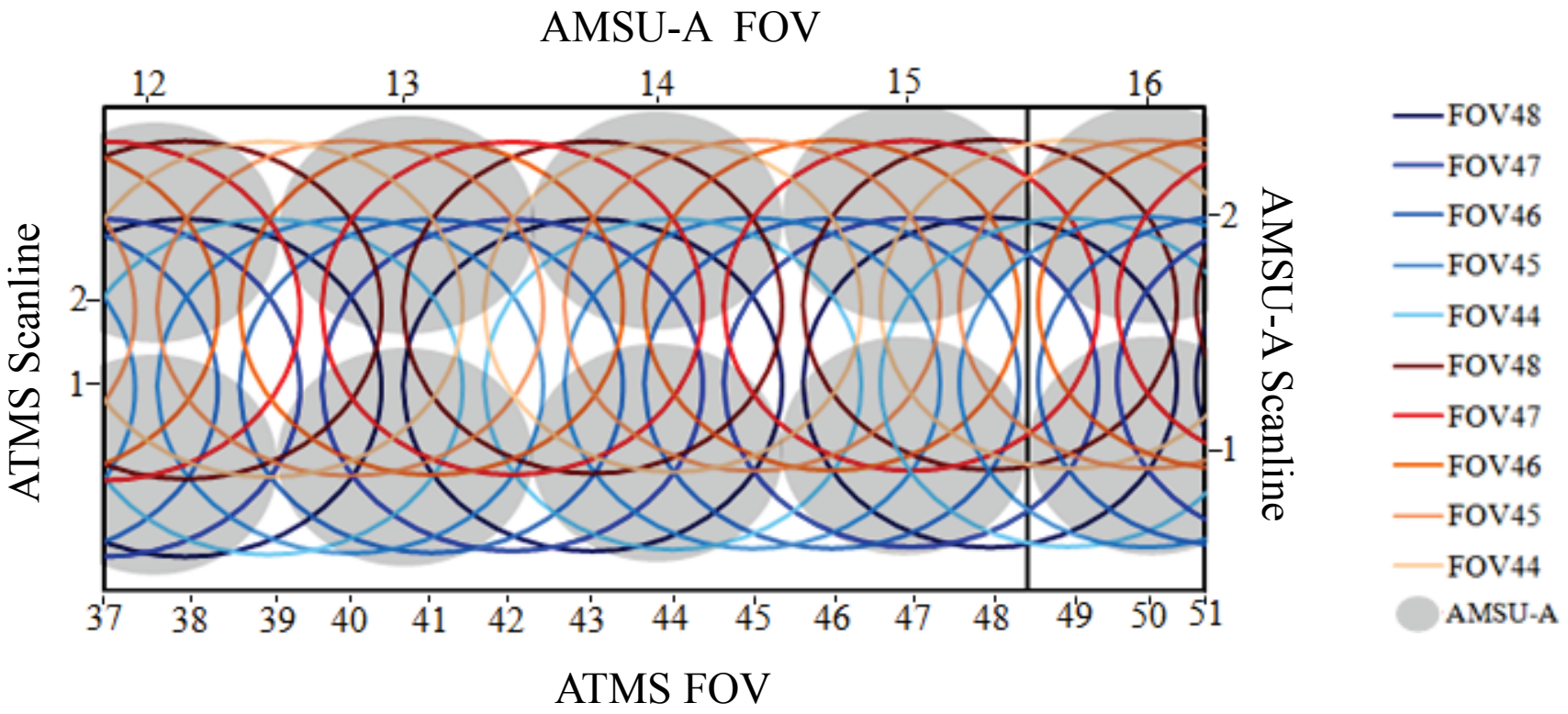

ATMS channels 1-2 beam width 5.2°
AMSU-A channels 1-2 beam width 3.3°

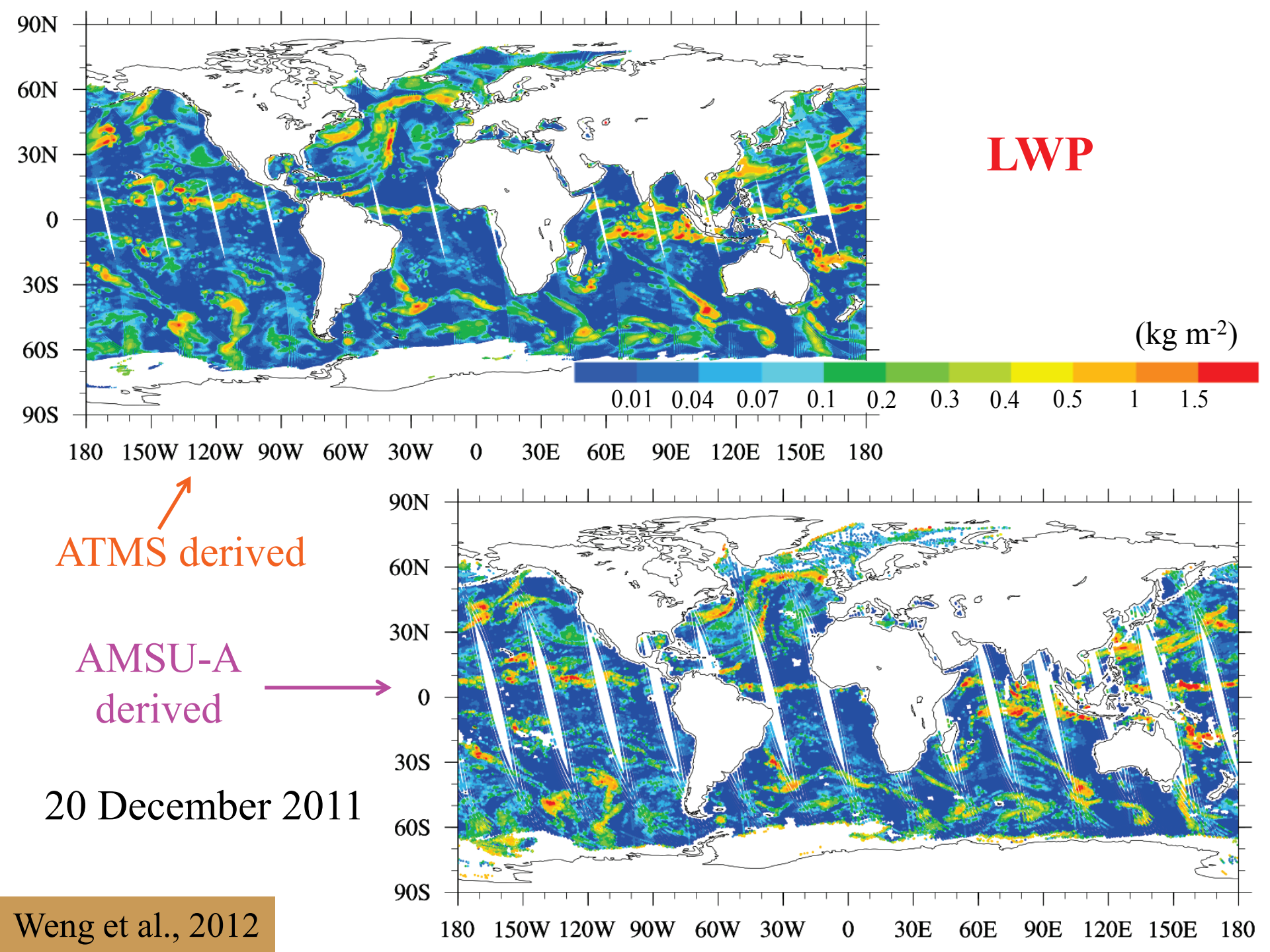
LWP
(kg m-2)
0.01 0.04 0.07 0.1 0.2 0.3 0.4 0.5 1 1.5
90N 60N 30N 0 30S 60S 90S
180 150W 120W 90W 60W 30W 0 30E 60E 90E 120E 150E 180
ATMS derived
AMSU-A derived
20 December 2011
Weng et al., 2012

The ATMS FOV Distribution along a Scanline

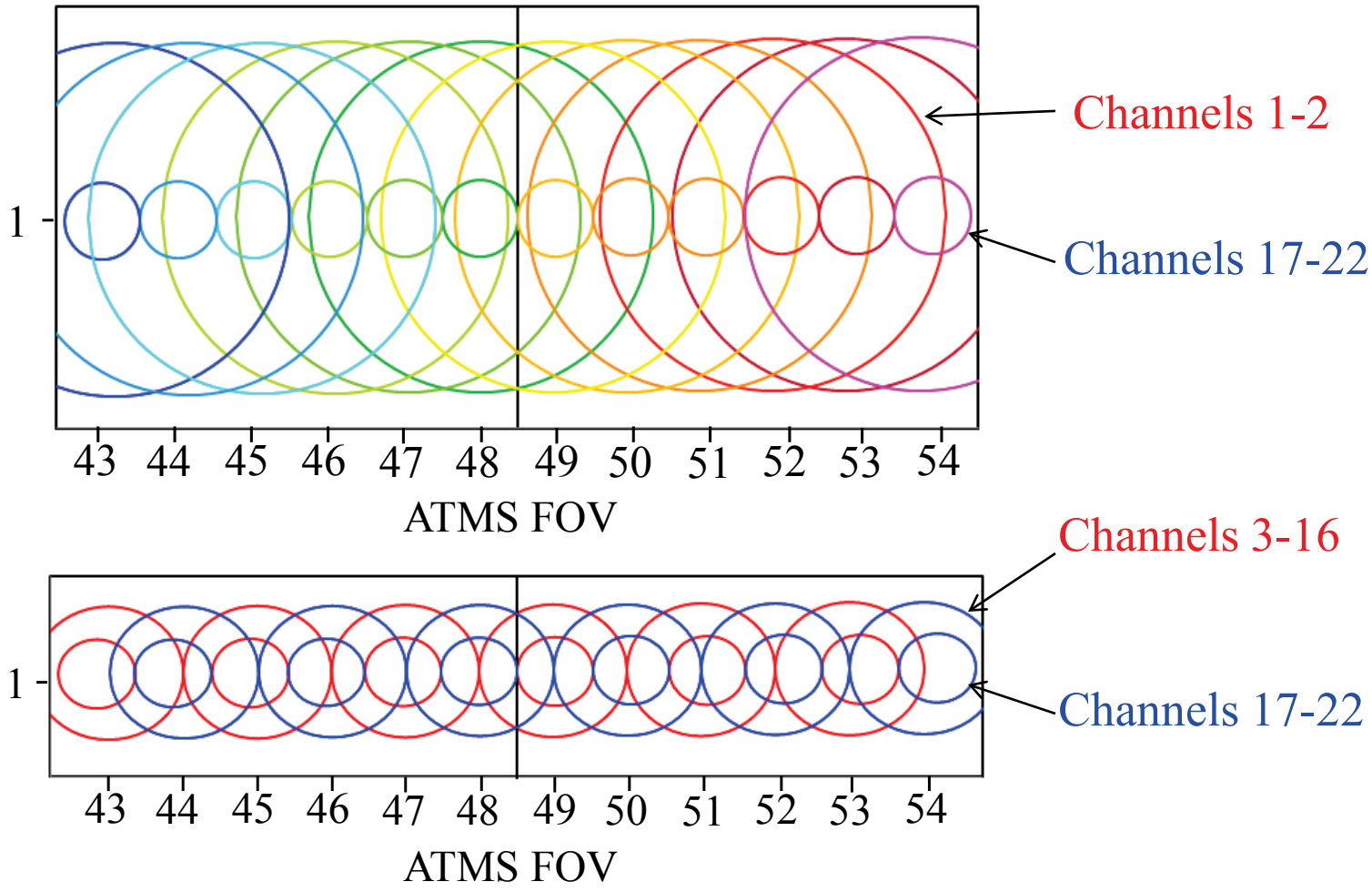

A consistent FOV distribution between temperature and humidity channels on ATMS makes the cloud detection easy to implement.

AMSU-A and MHS FOVs

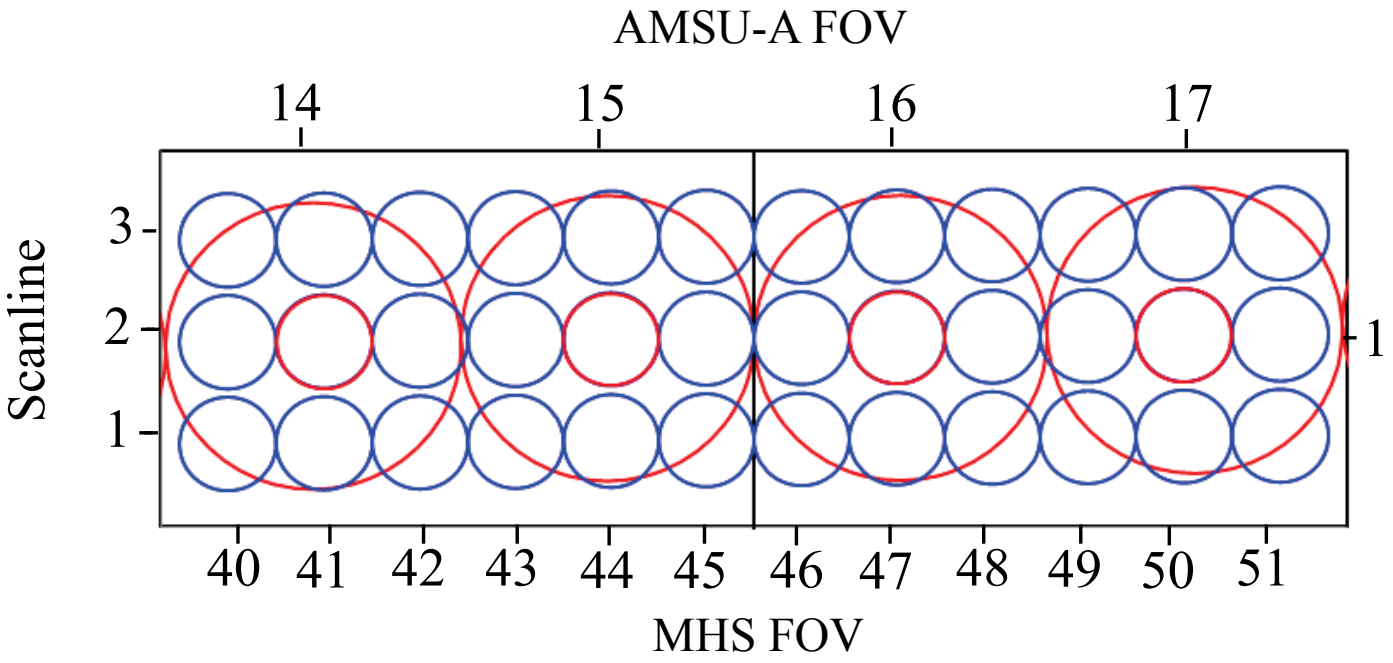

An inconsistent FOV distribution between AMSU-A and MHS channels makes MHS cloud detection extremely challenging.

Comparison of FOV Distributions between ATMS and AMSU

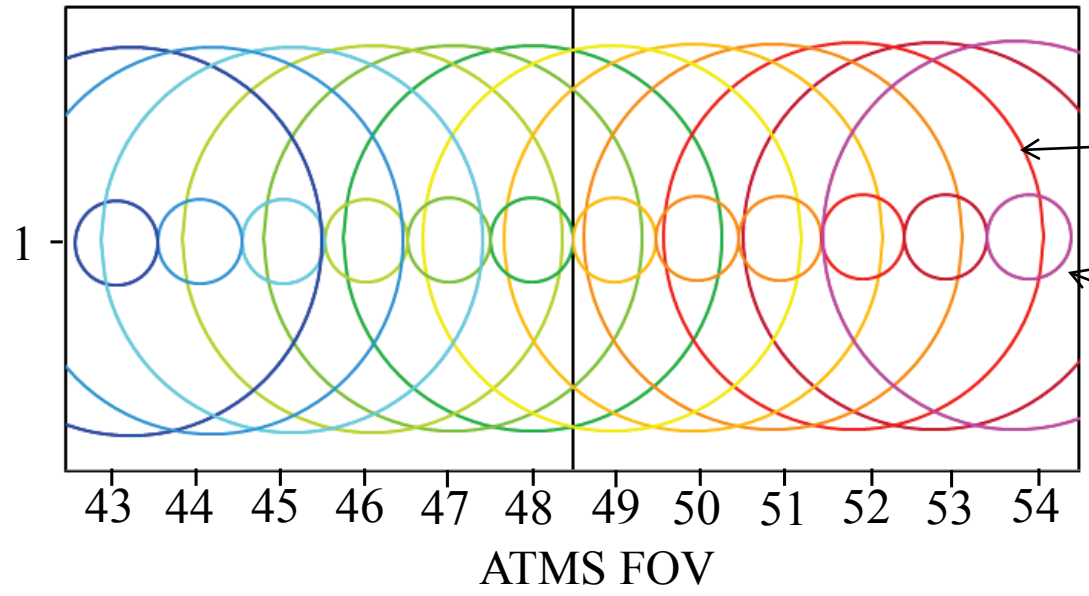

ATMS Channels 1-2

ATMS Channels 17-22

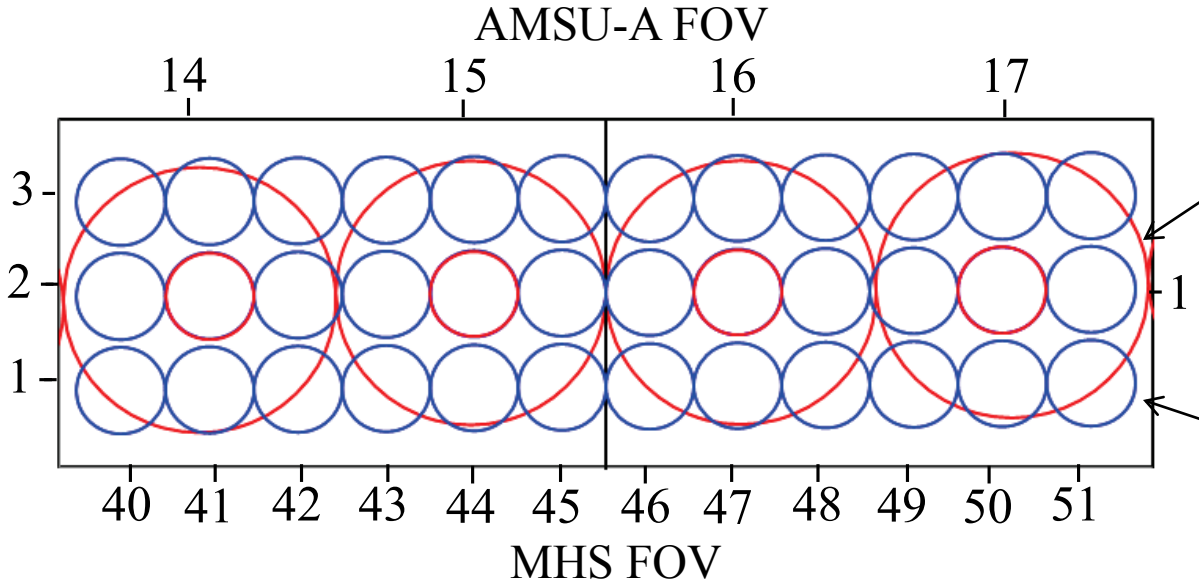

AMSU-A Channels 1-2

MHS Channels 1-5

LWP (AMSU-A channels 1-2)

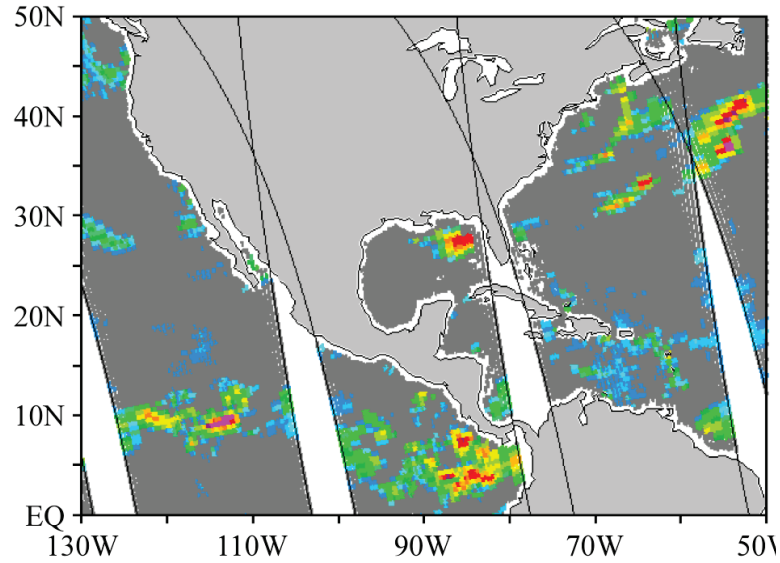

IWP (MHS channels 1-2)

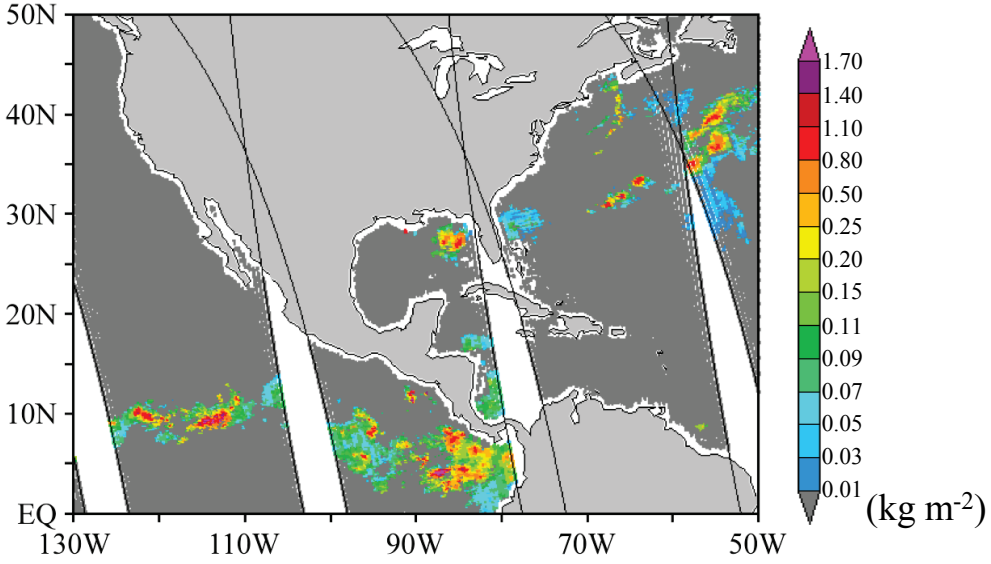

T_b (GOES-12, 10.7μm channel)

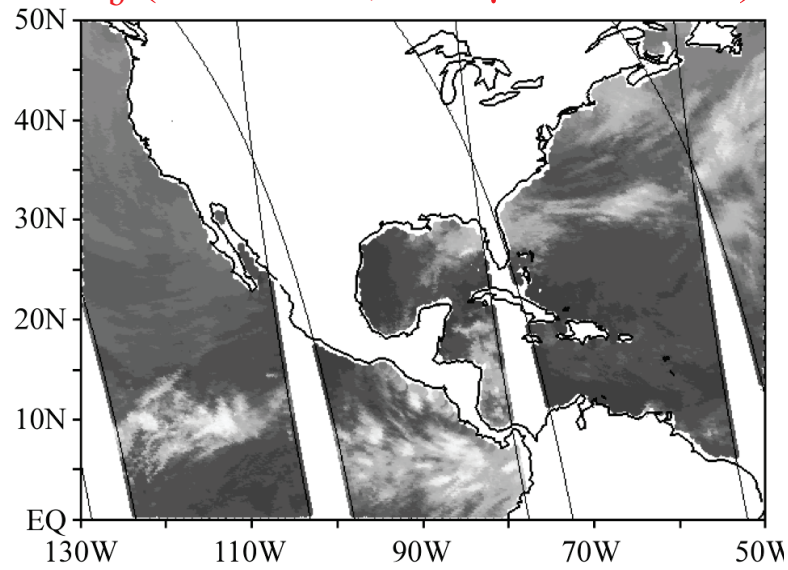

LWP/IWP Collocation

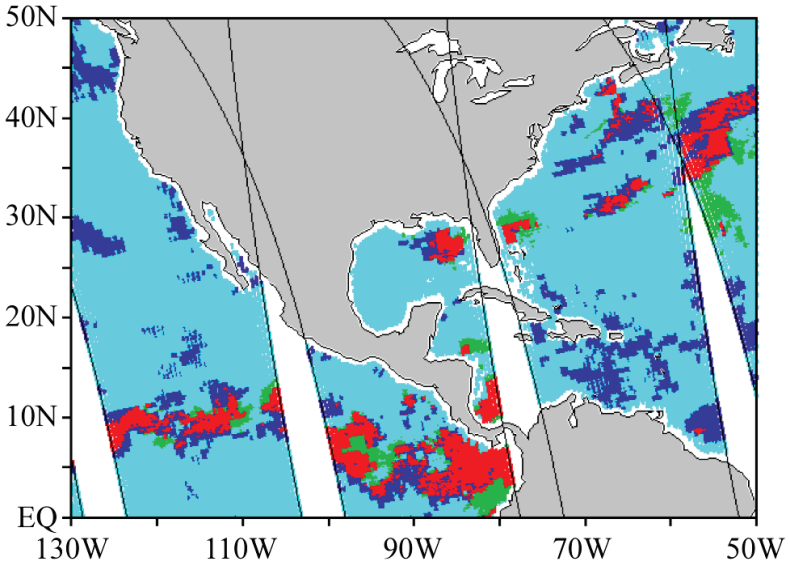

clear-sky
warm cloud
ice cloud
mixed-phase cloud

NOAA-18, 1441 UTC to 2303 UTC on May 22, 2008

Impact of Model Top Altitude on Satellite Data Assimilation for TC Forecasts

ATMS Channels

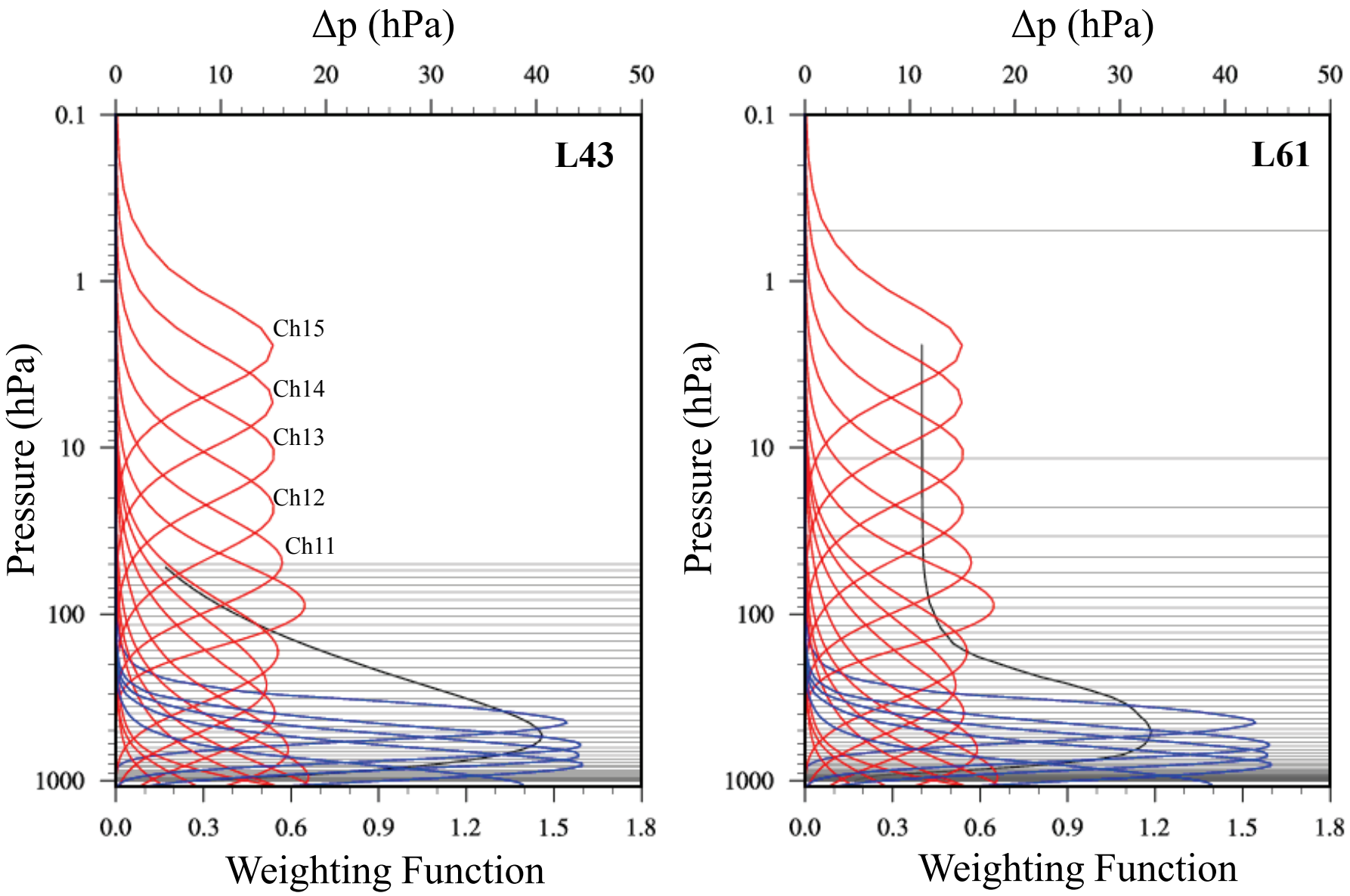

AMSU-A Channels

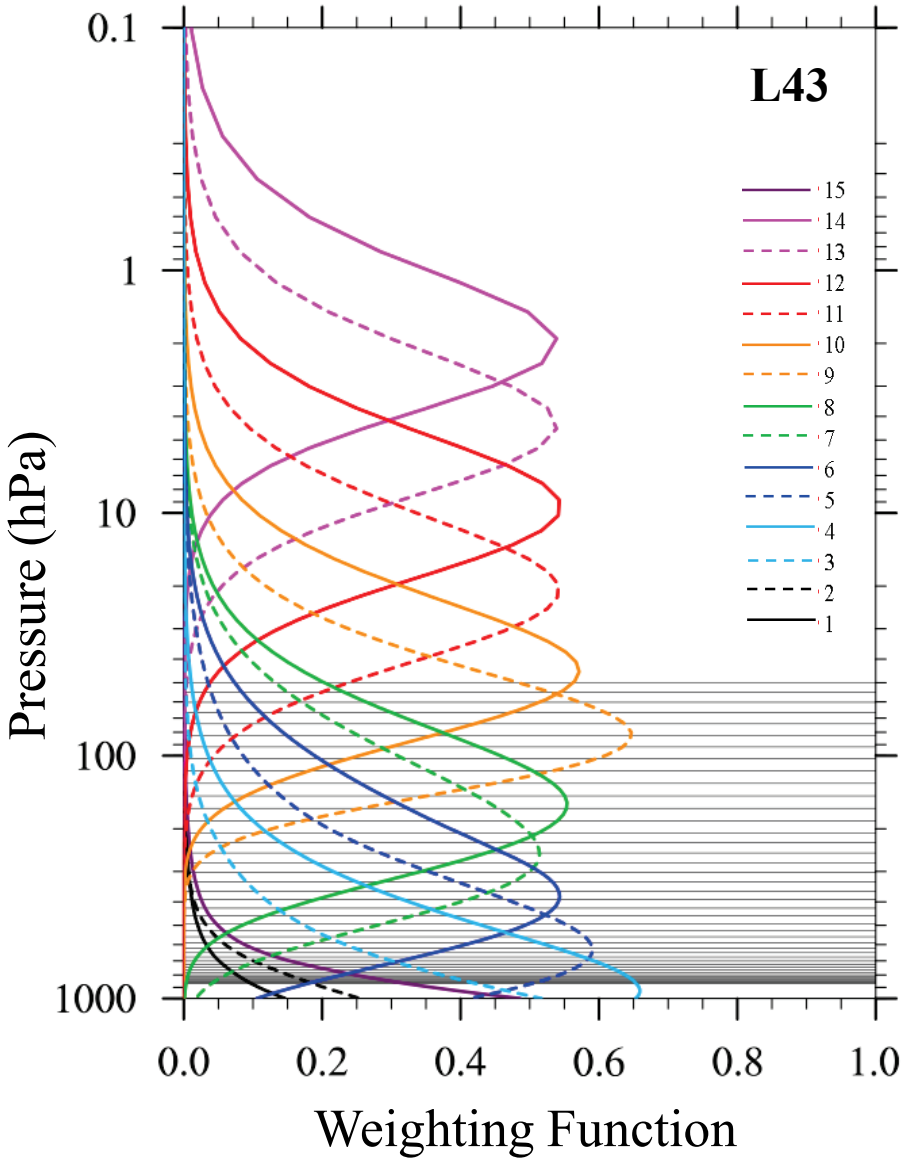

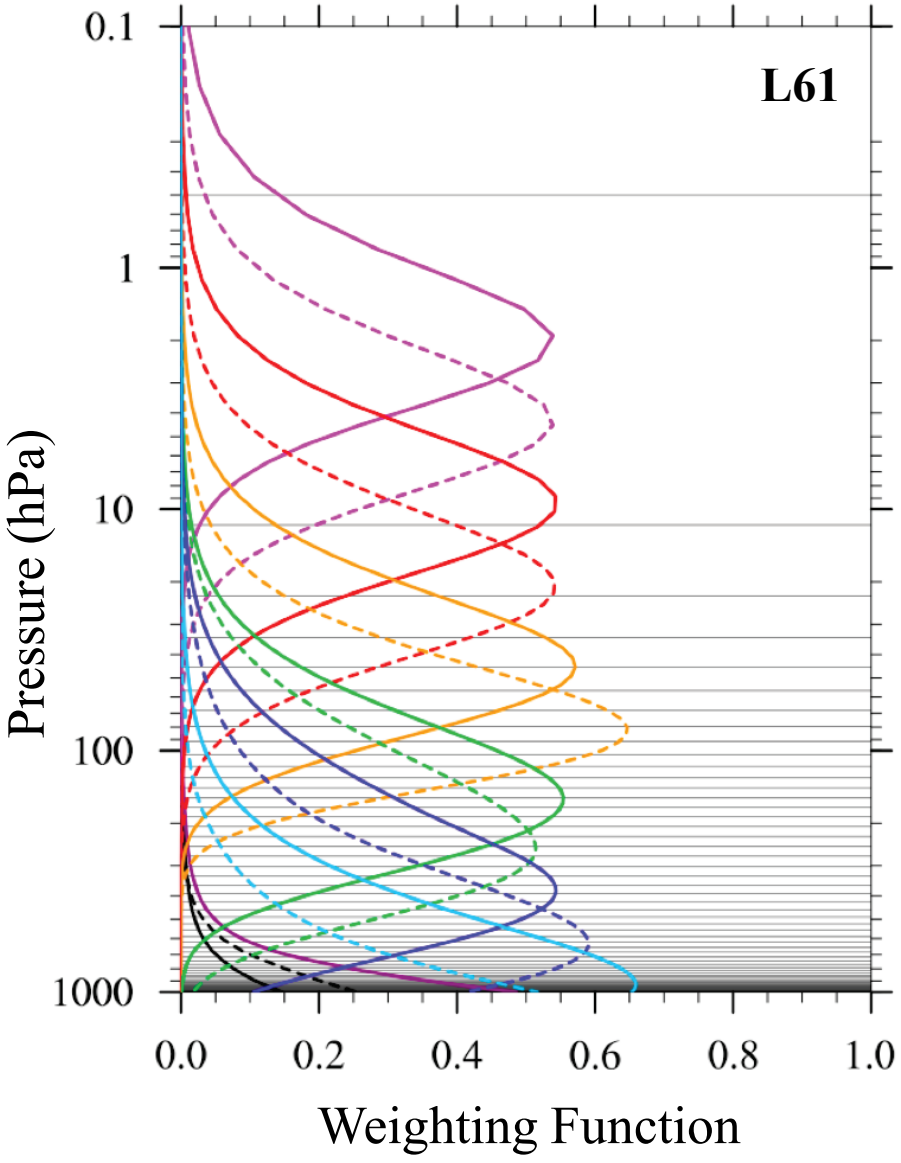

HIRS Channels

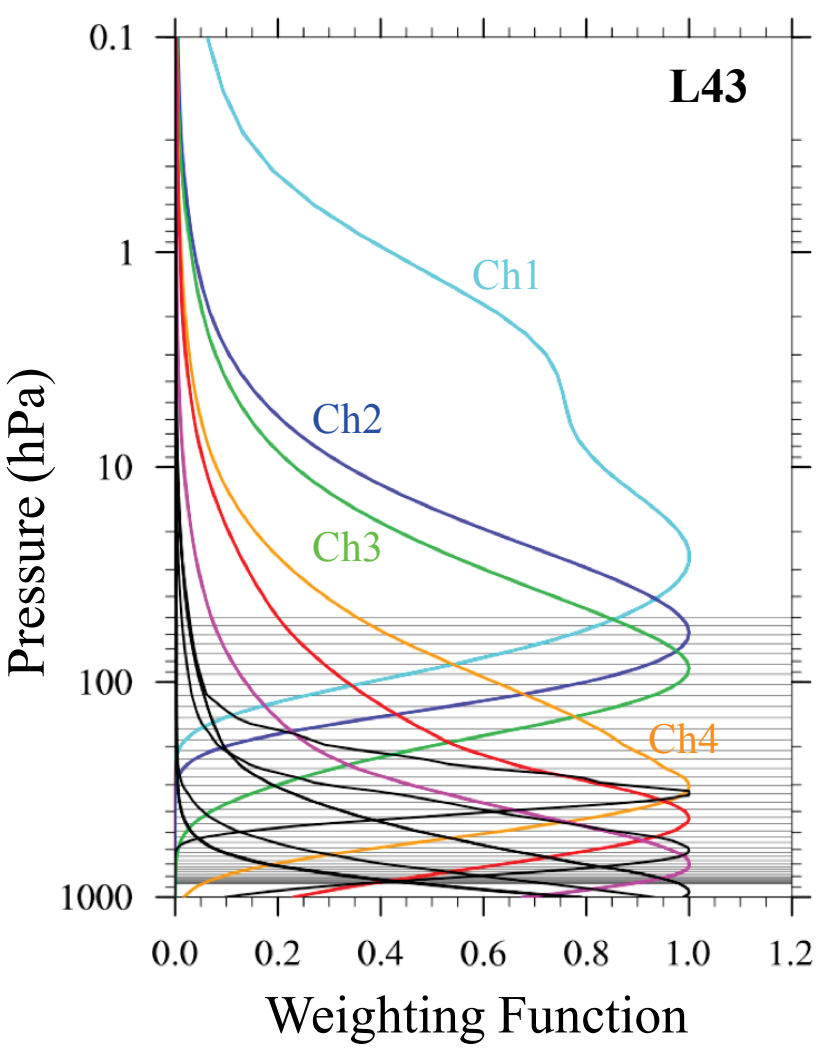

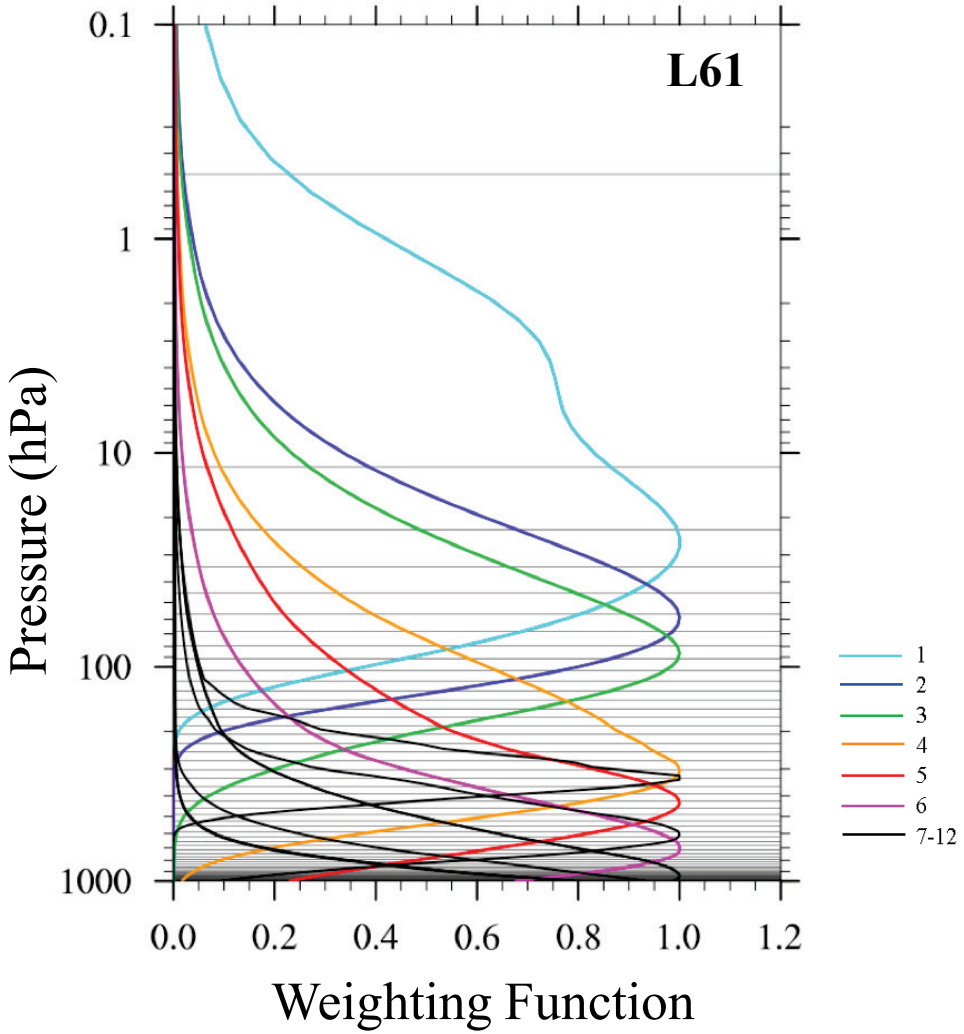

AIRS Channels (281)

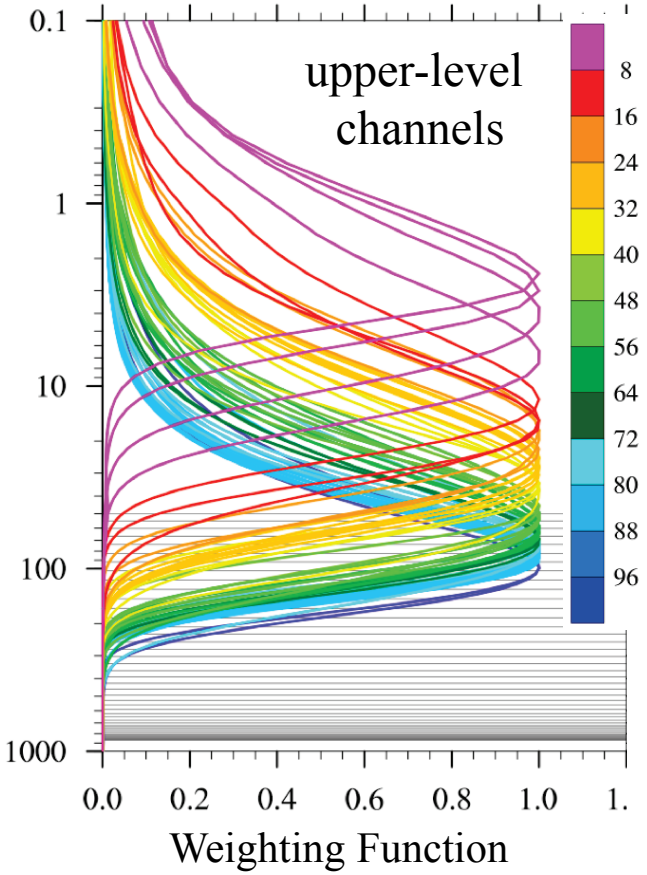

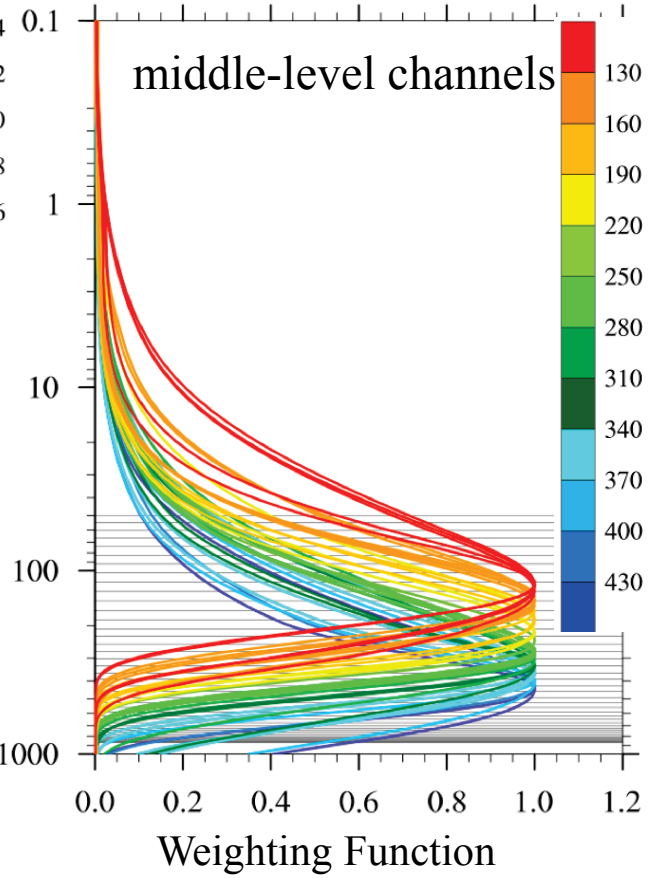

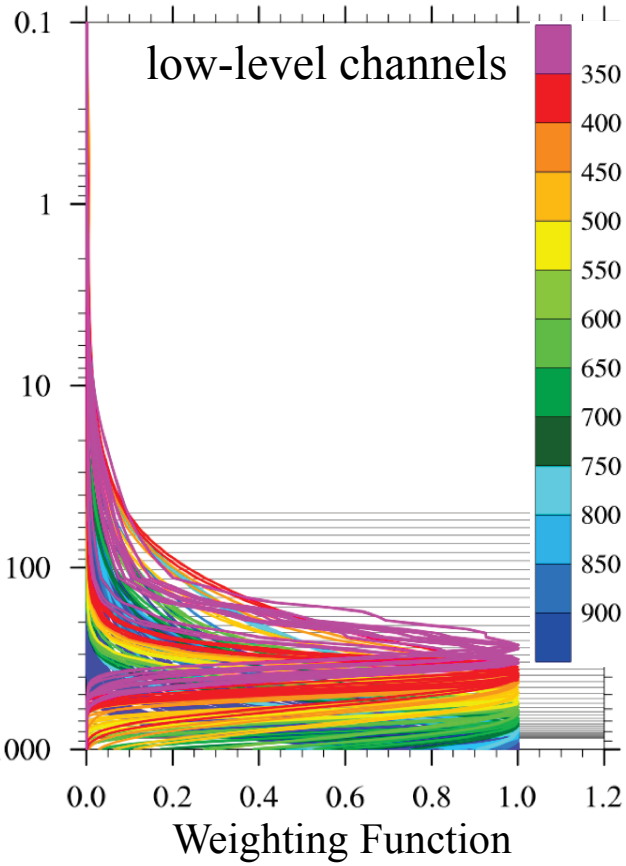

These 281 channels are selected for data assimilation in the GSI/HWRF system. The pressure at which WF reaches a maximum is indicated in color.

The Best Track of Four 2012 Atlantic Landfall Hurricanes Selected for This Study

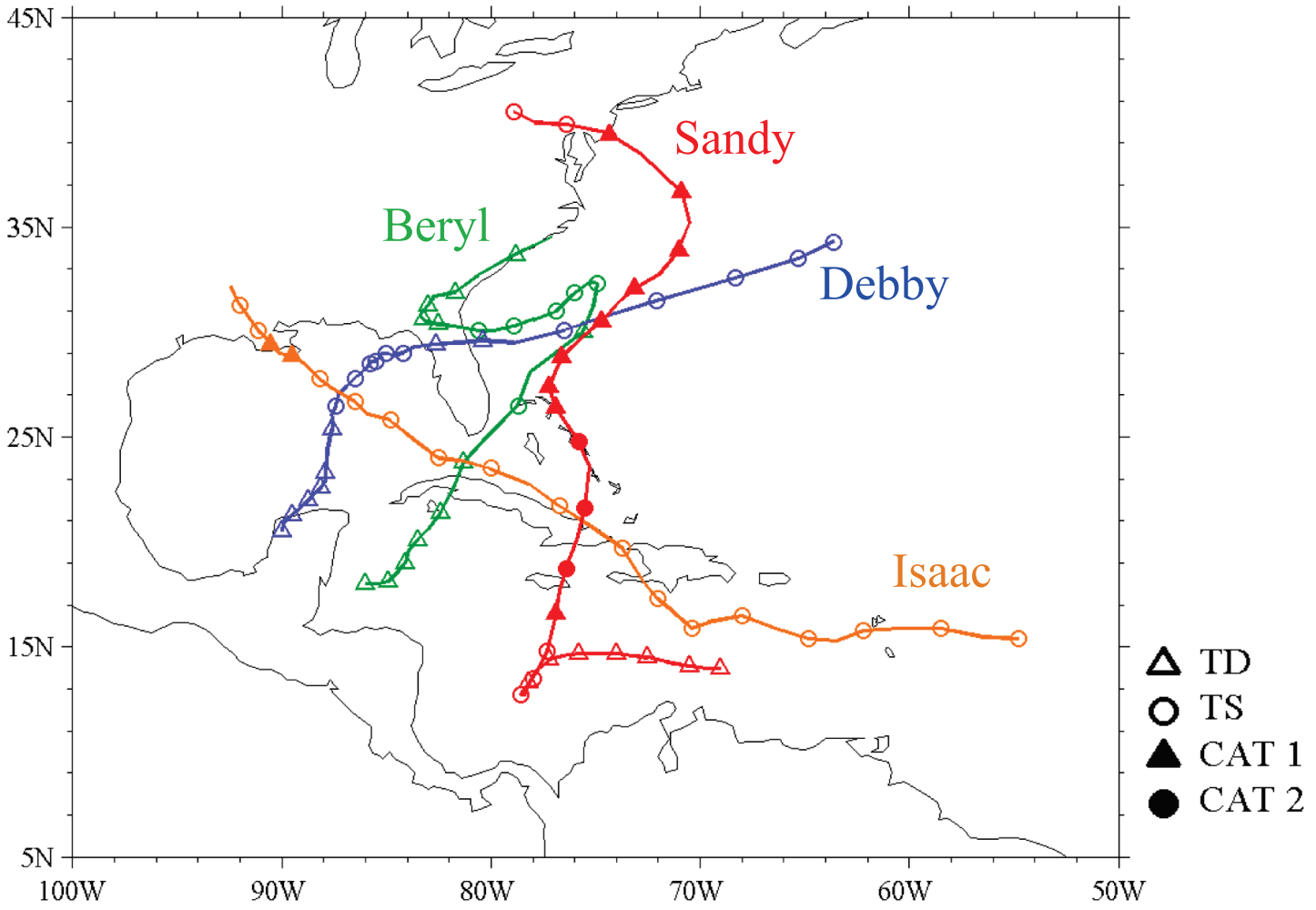

Track Predictions of the 2012 Operational HWRF

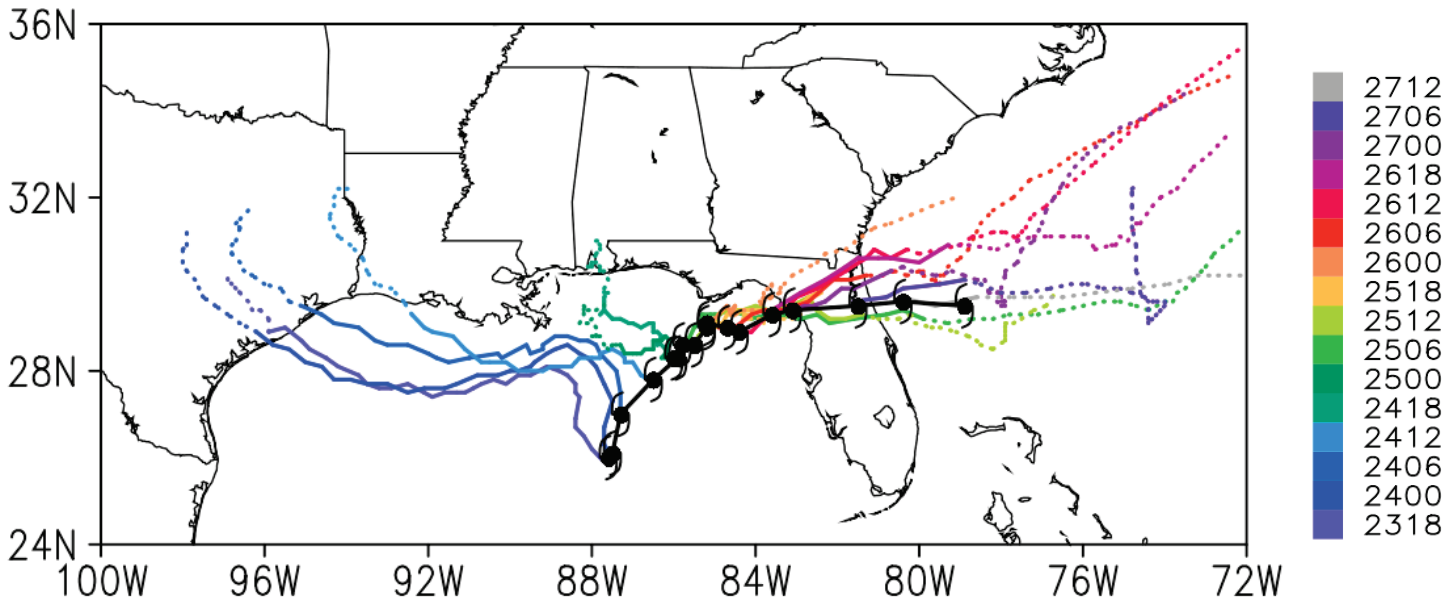

- The operational HWRF model produced an eastward propagating tracks while Debby moved northeastward when model forecasts were initialized before June 25, 2012
- The operational HWRF model produced reasonably good track forecasts after June 25 and afterward.

The track prediction of Debby before June 25, 2012 was a major challenge.

500-hPa Geopotential and Wind Vector Distributions

1200 UTC
June 23 ,2012

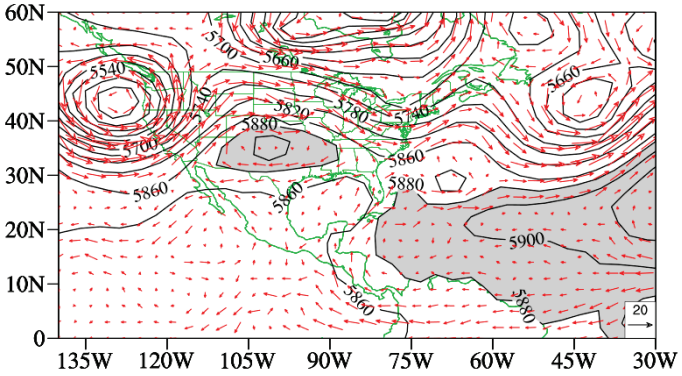

1800 UTC
June 23, 2012

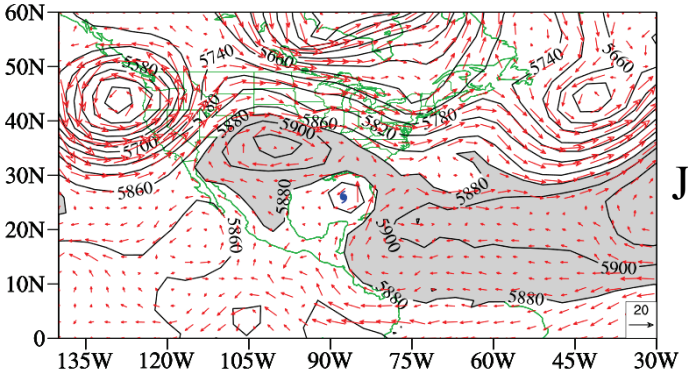

0000 UTC
June 24 ,2012

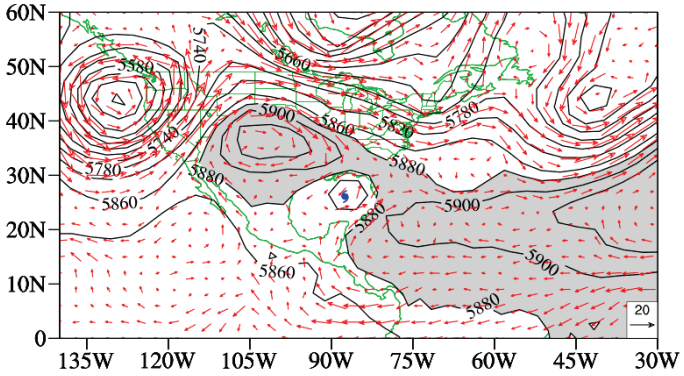

0600 UTC
June 24, 2012

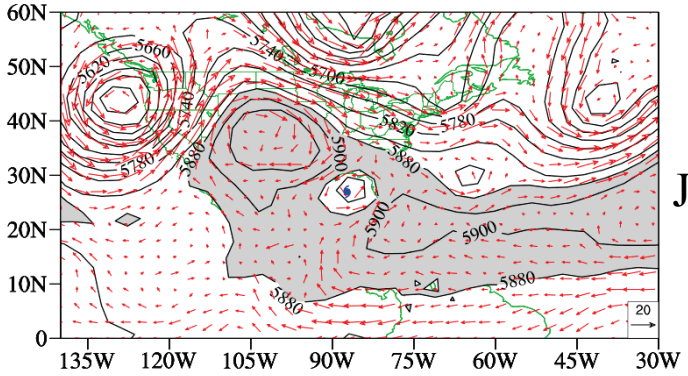

1200 UTC
June 24, 2012

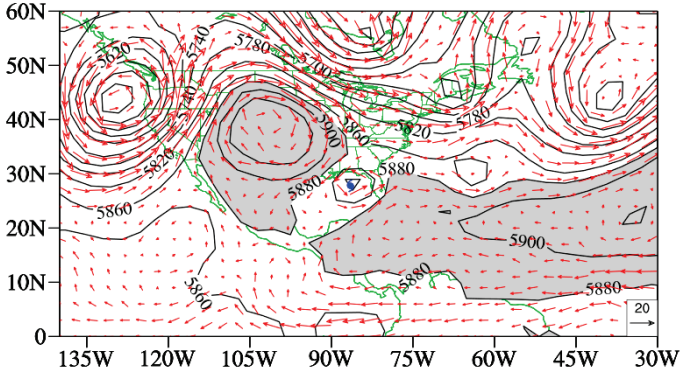

1800 UTC
June 24, 2012

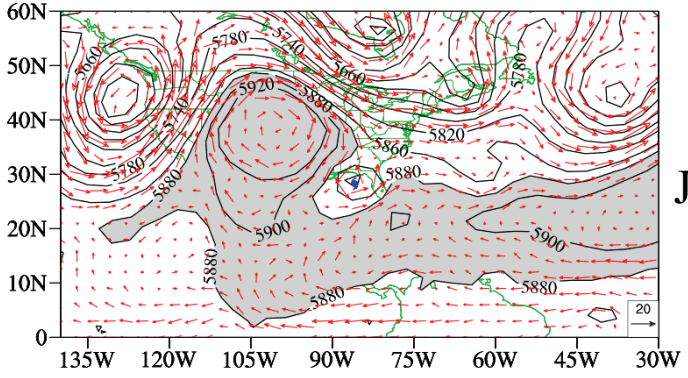

HWRF Domain Sizes for Tropical Storm Debby

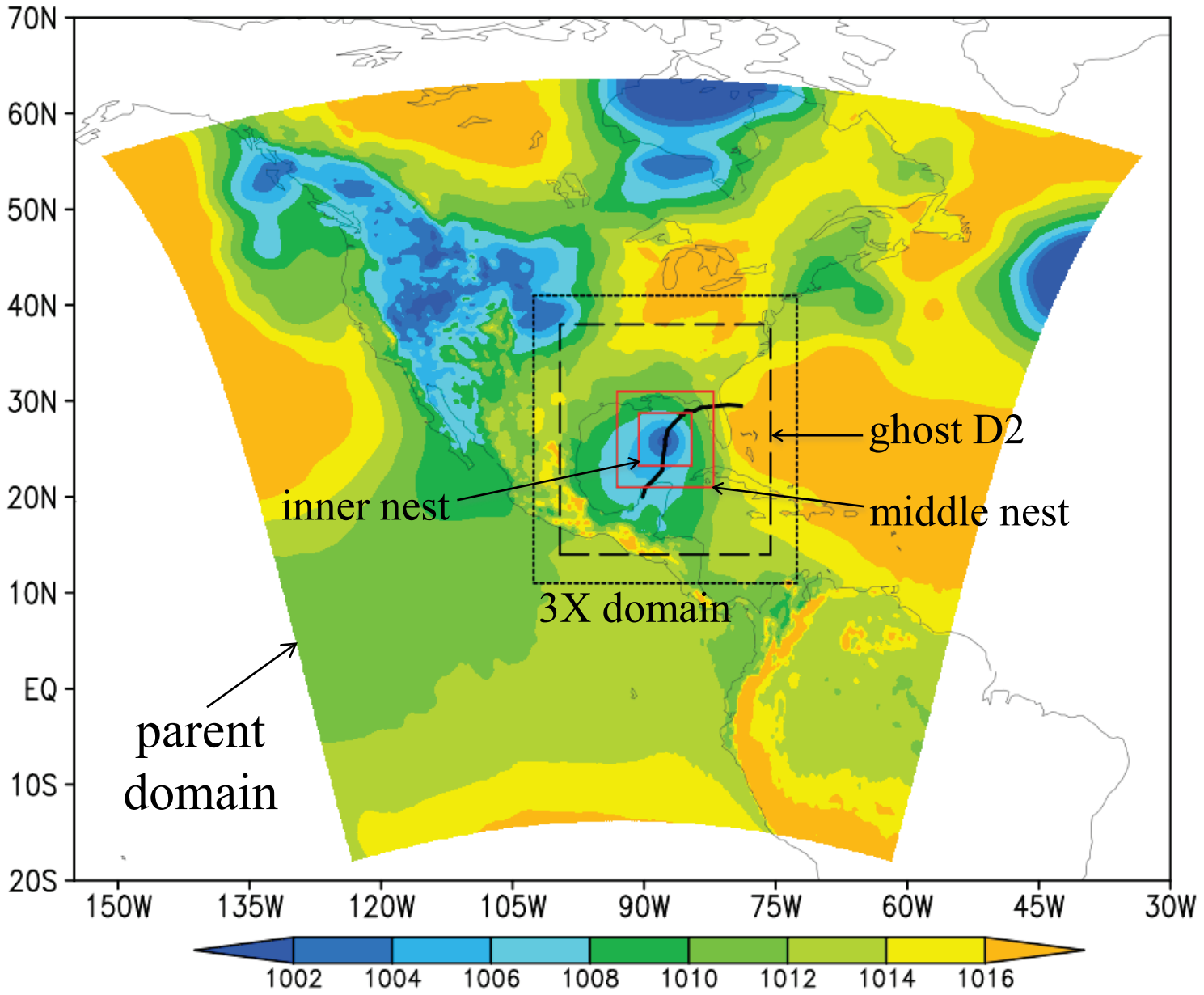

UTC Dependence of Polar-Orbiting Satellite Data

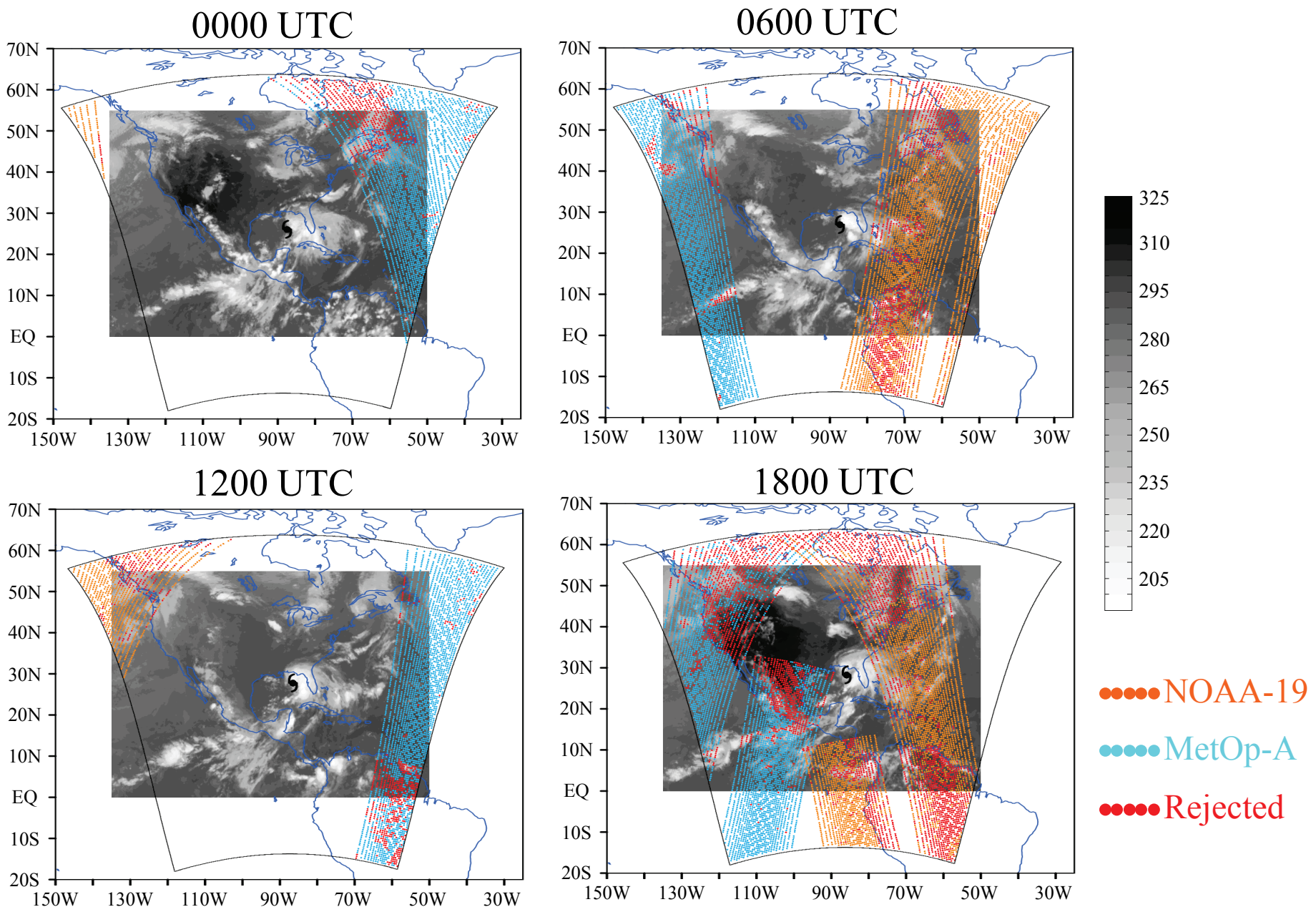

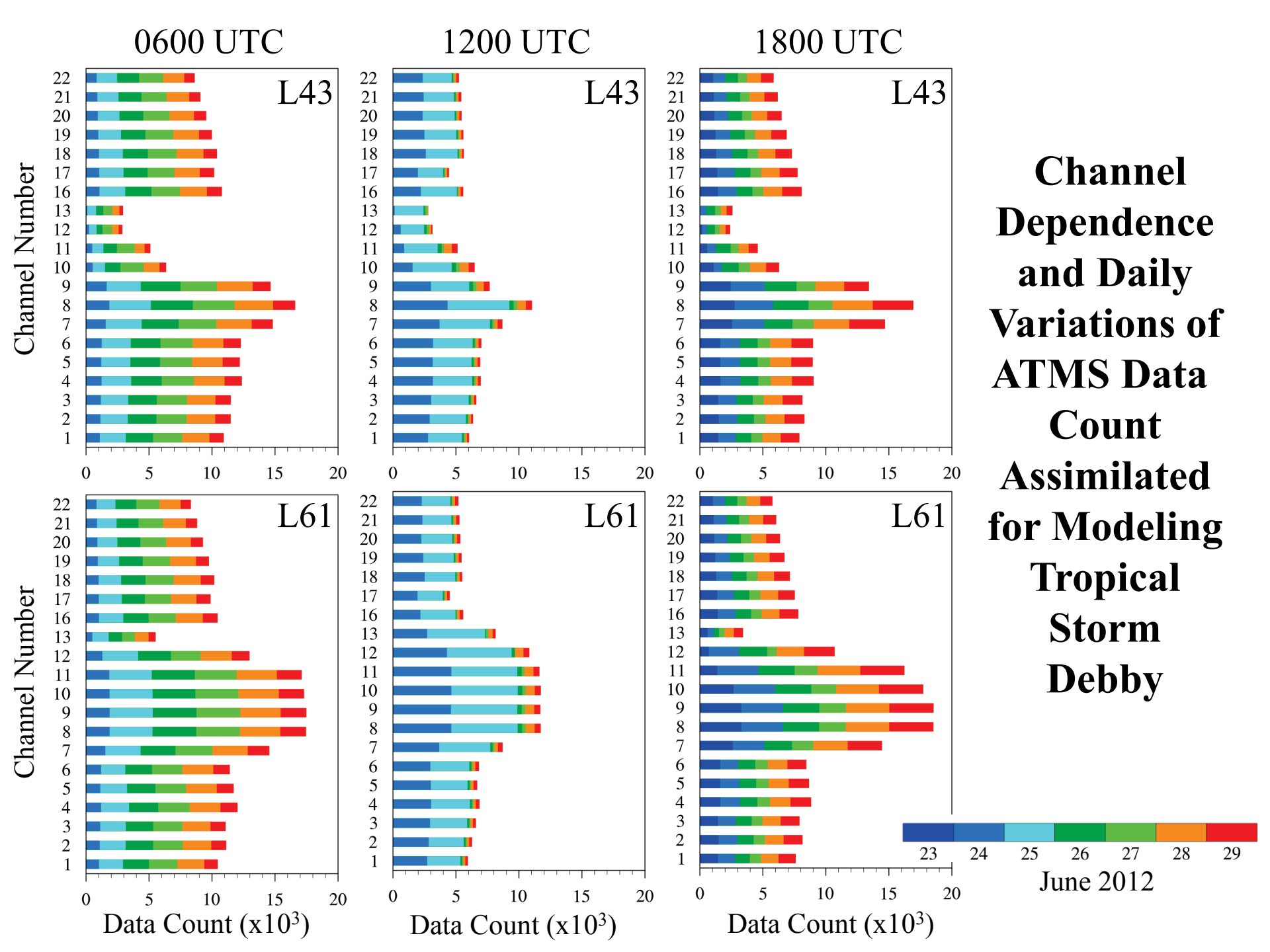
0600 UTC
1200 UTC
1800 UTC
L43
L61
Channel Number
Data Count (x10³)
0
5
10
15
20
23
24
25
26
27
28
29
June 2012
Channel Dependence and Daily Variations of ATMS Data Count Assimilated for Modeling Tropical Storm Debby

AIRS Channel Dependence of Data Count Assimilated During Tropical Storm Debby

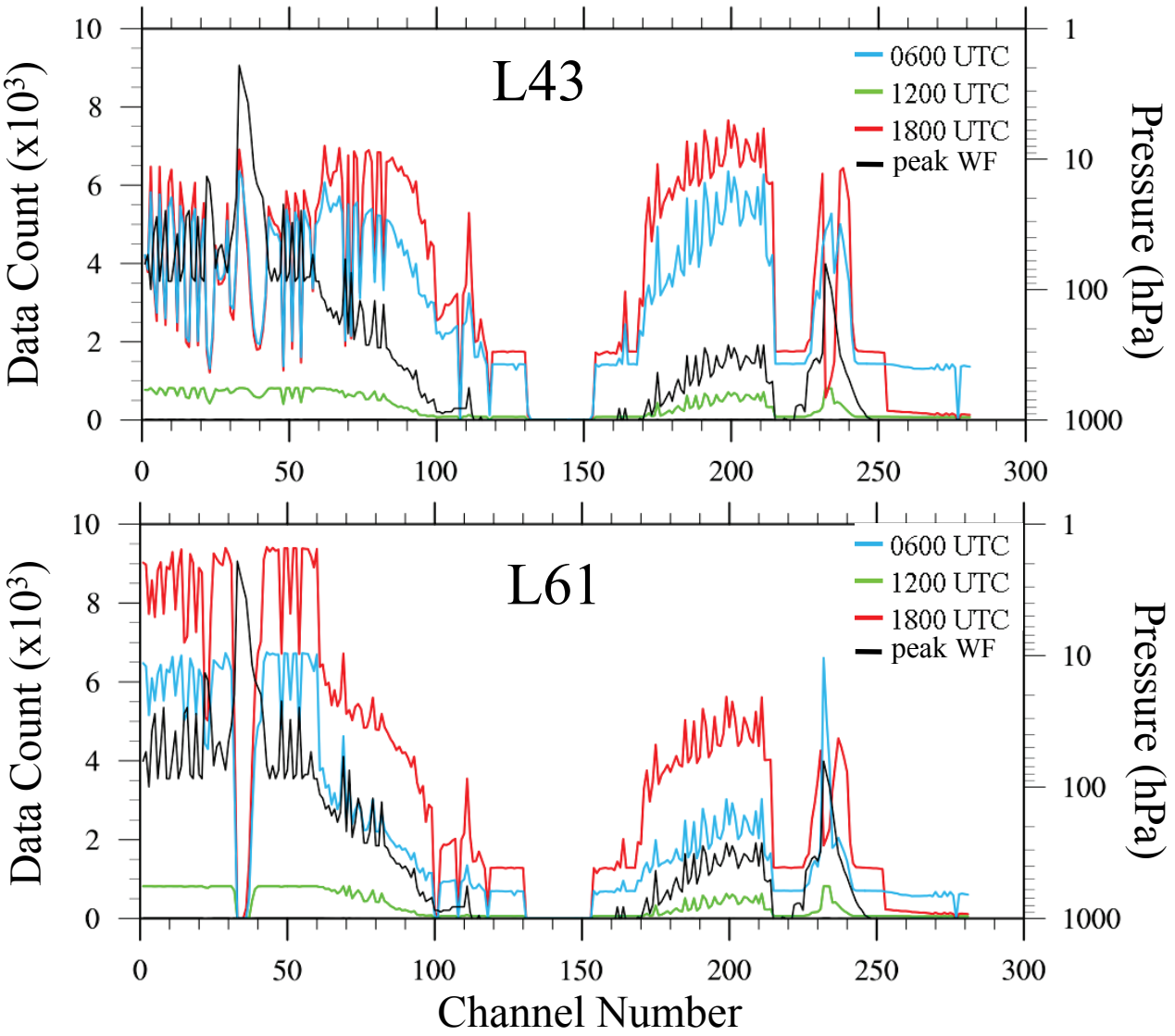

More upper-level channel data are assimilated in L61 with a higher model top (0.5 hPa) than L43 whose model top is located around 50 hPa.

O-B and O-A Distributions of ATMS Upper-Level in L61

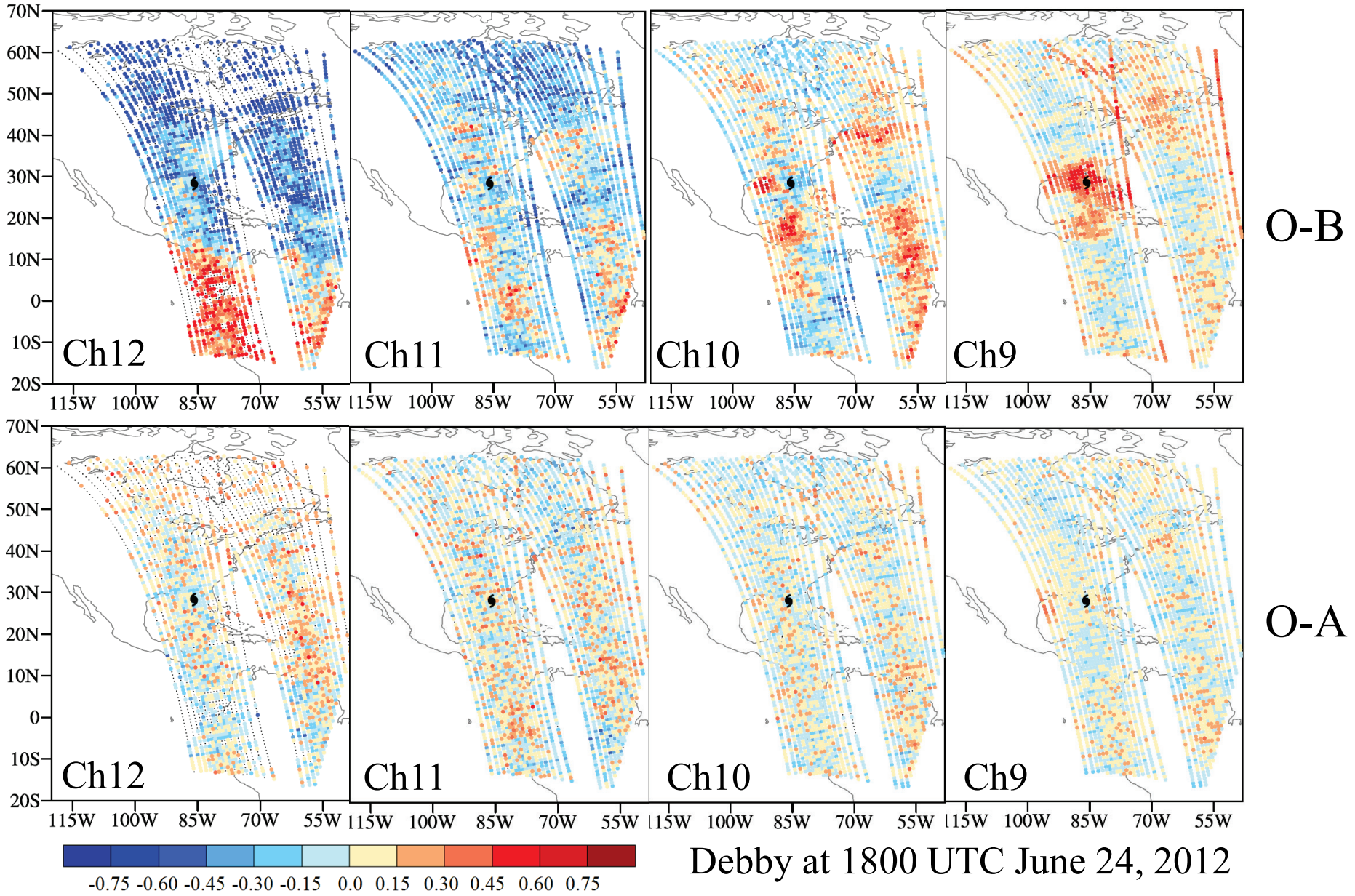

O-B and O-A Distributions of ATMS Upper-Level in L43

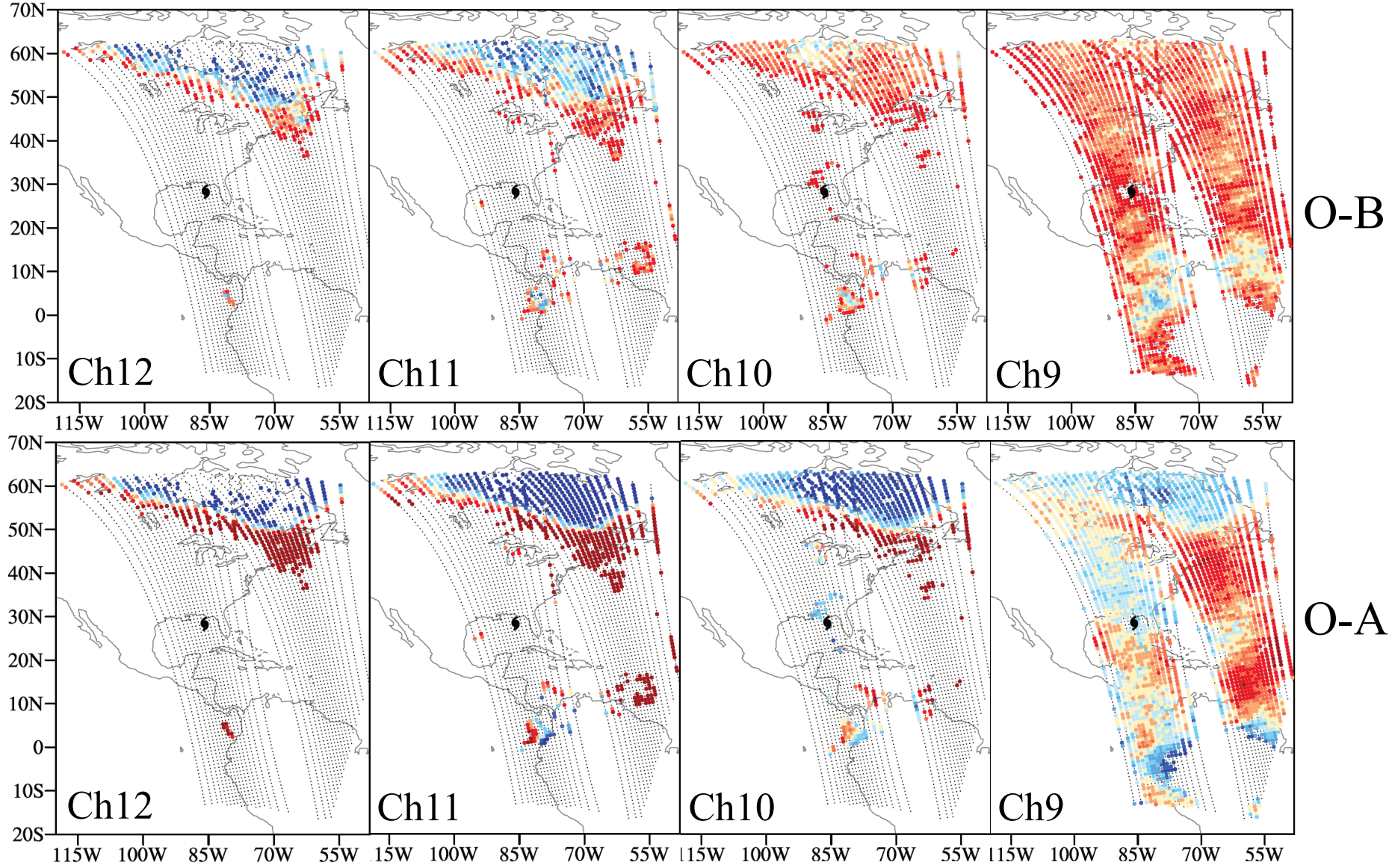

Debby at 1800 UTC June 24, 2012

Model Fit to AIRS Observations before and after DA

L43

L61

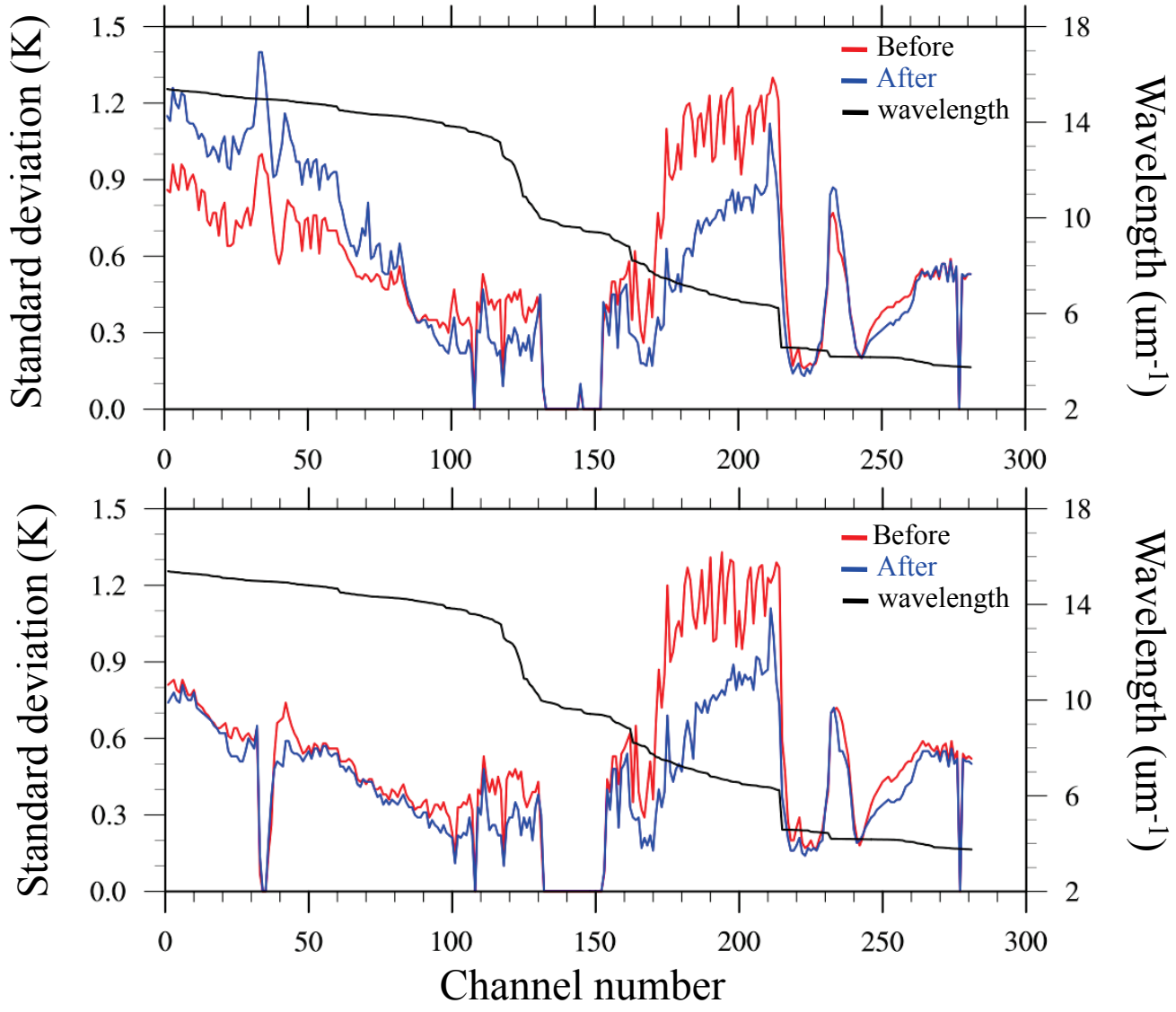

The std. of O-A is greater than that of O-B for upper-level channels in L43.

Comparison of Track Forecasts between L61 and L43

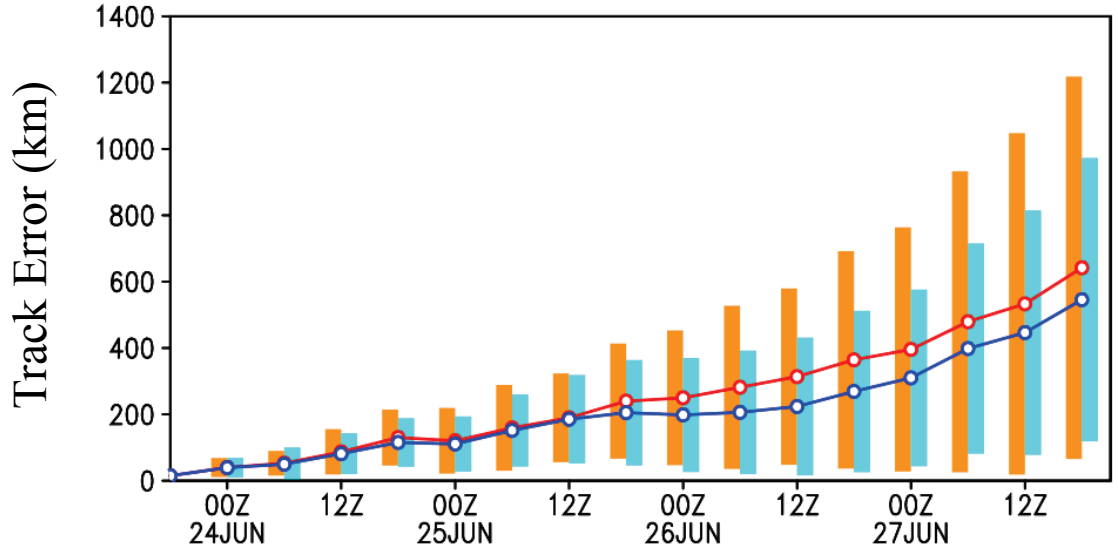

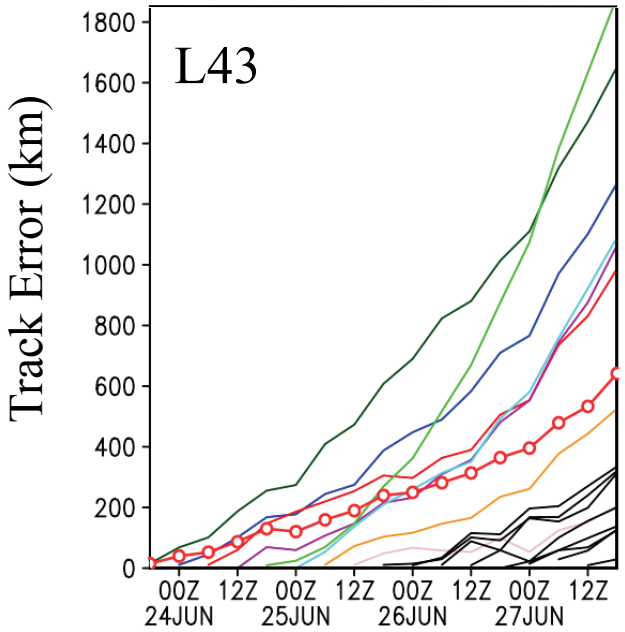

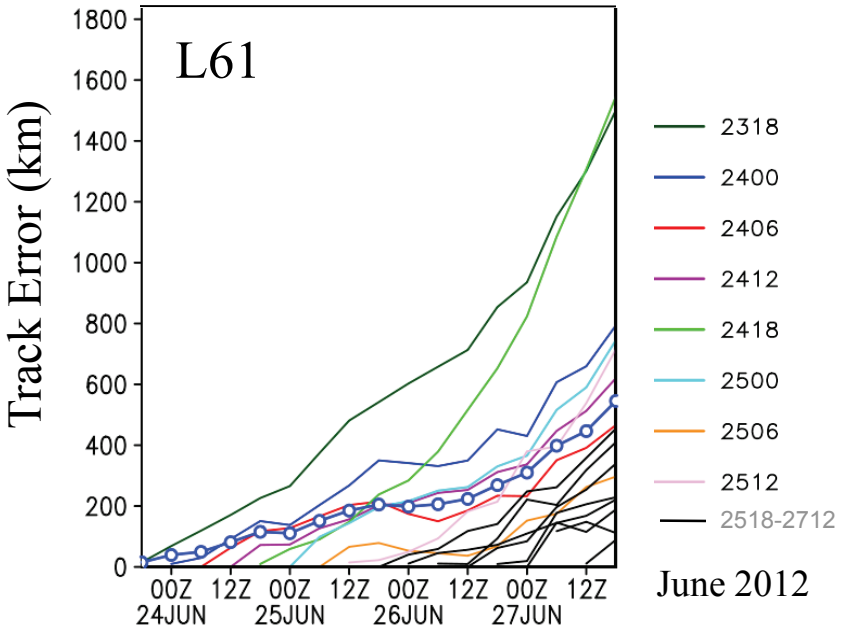

June 2012

Track Prediction for Tropical Storm Debby

L43

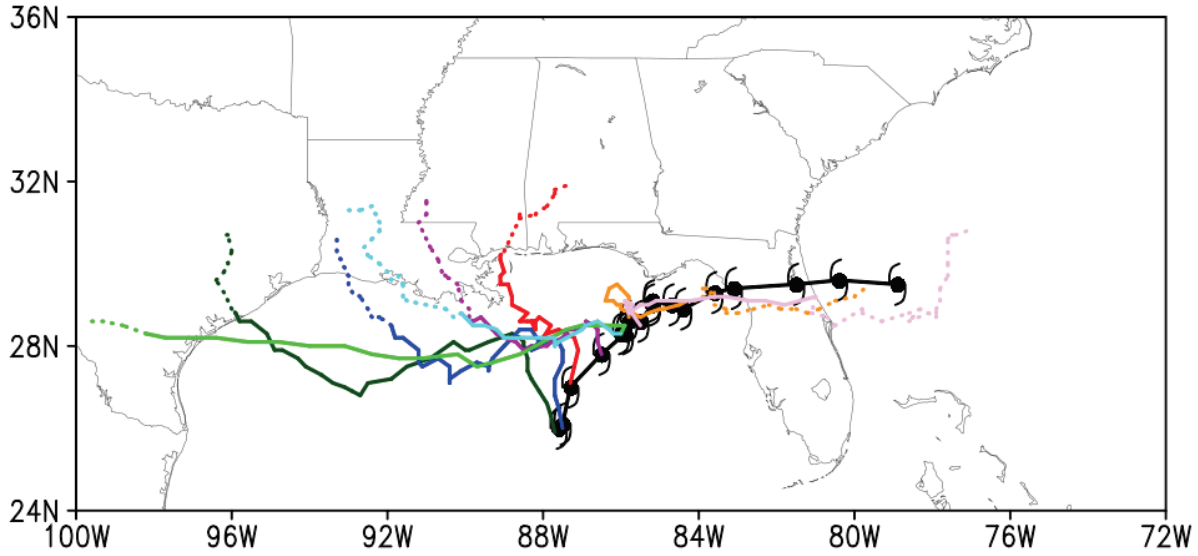

L61

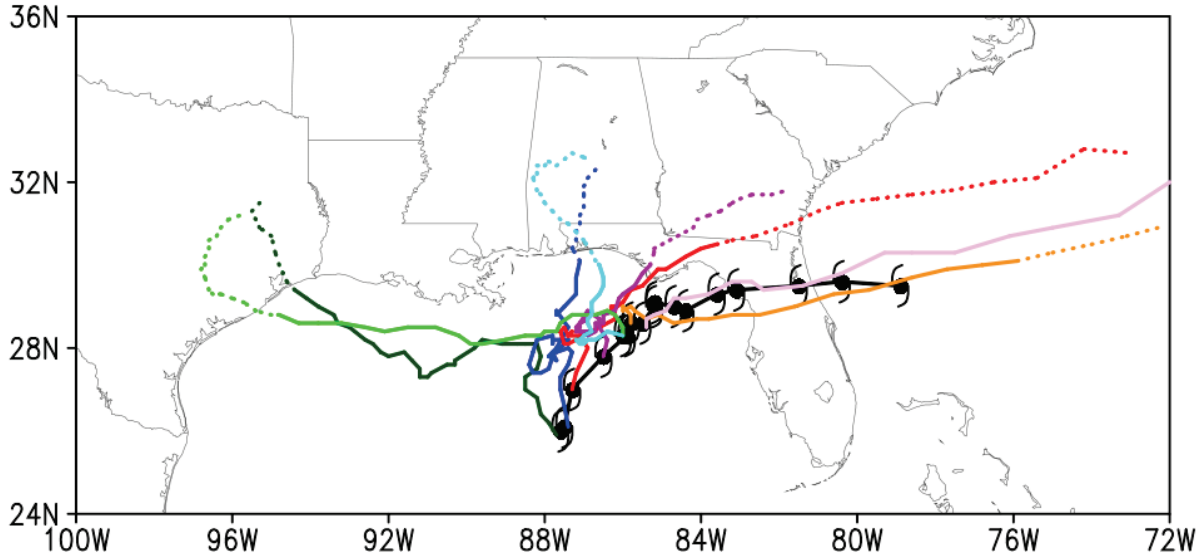

2318
2400
2406
2412
2418
2500
2506
2512

June 2012

Geopotential and Wind Vector Valid at 1800 UTC June 24, 2012 in L61 Experiment

Analysis

6-h Forecast

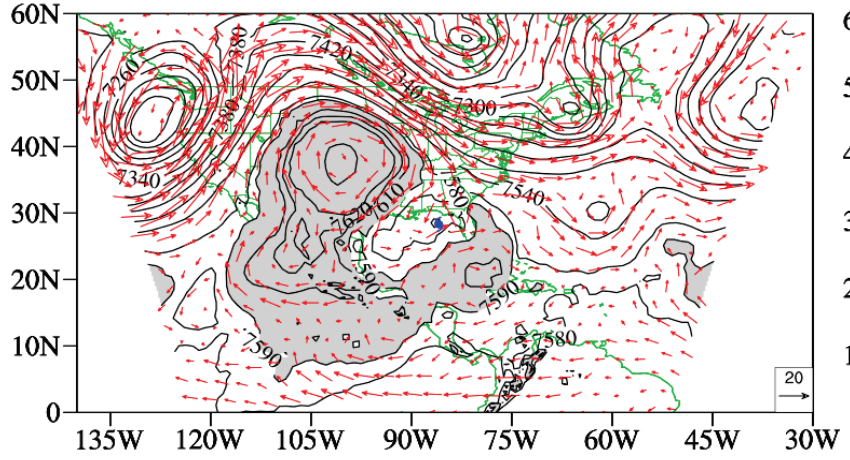

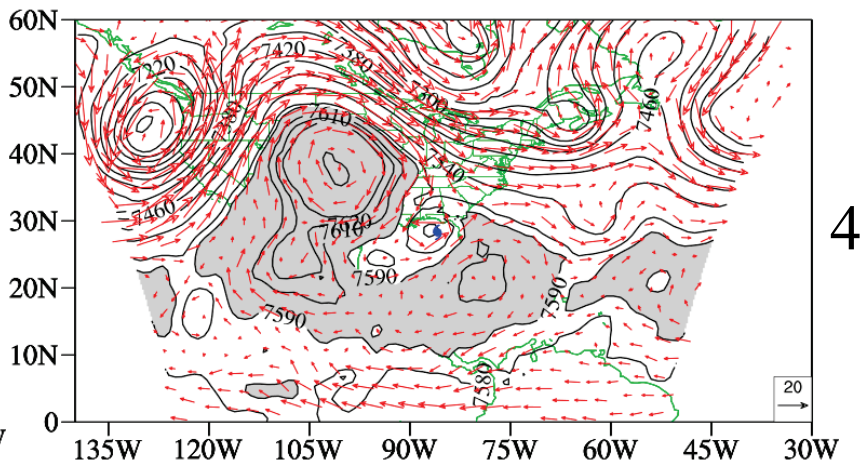

400 hPa

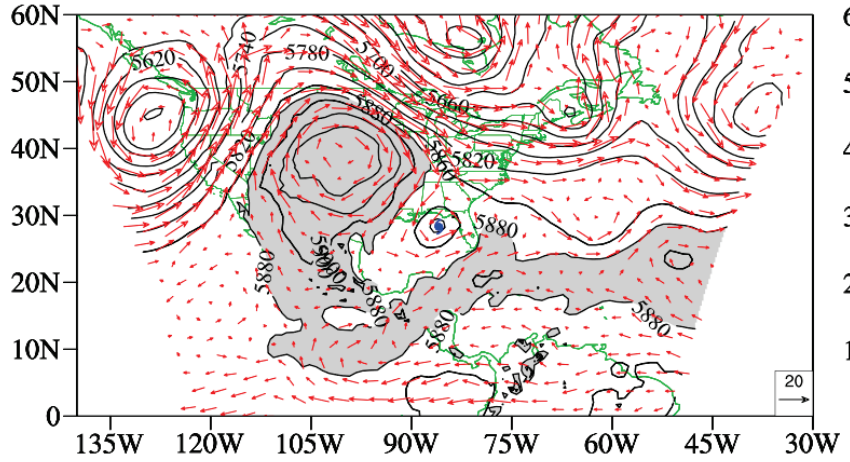

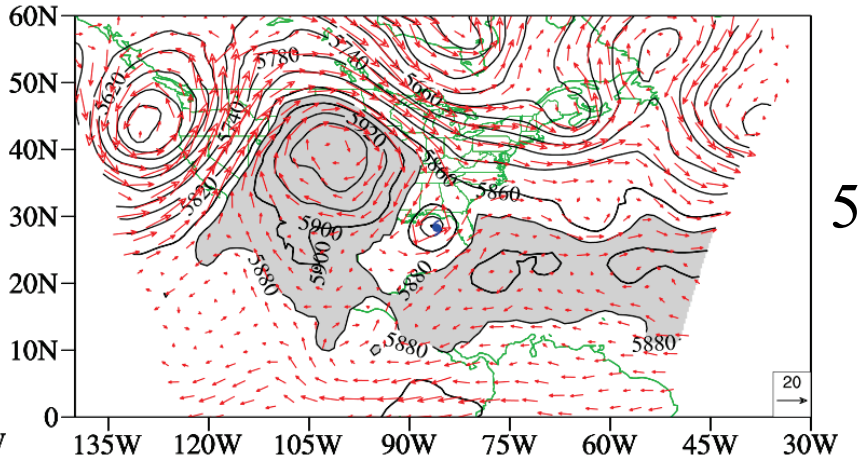

500 hPa

Steering Flow Derived from the L61 Model Forecasts Initialized at 1200 and 1800 UTC June 24, 2012

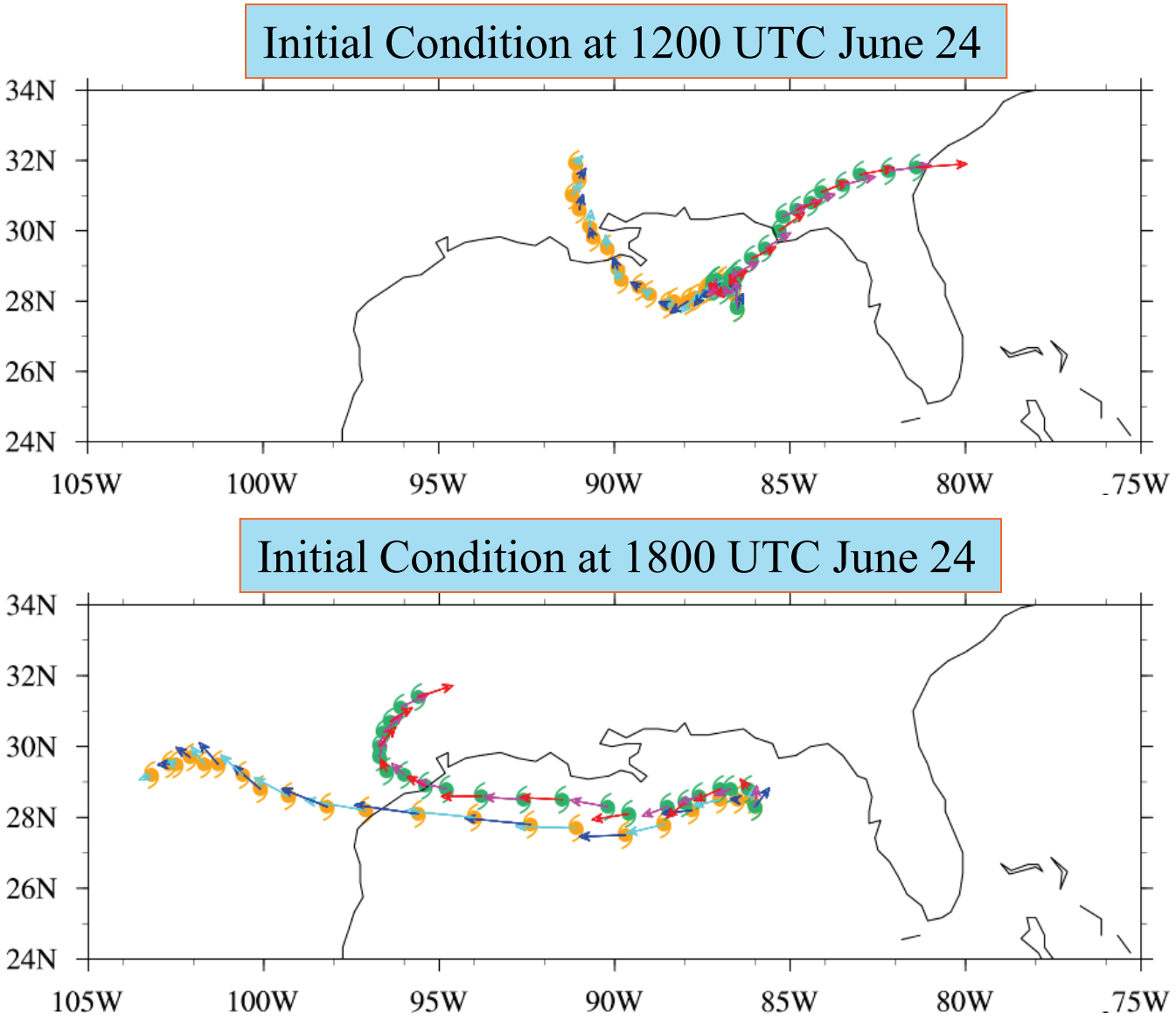

Mean Forecast Errors for Four 2012 Atlantic Hurricanes

Impact of Model Top Altitude on Track and Intensity Forecasts

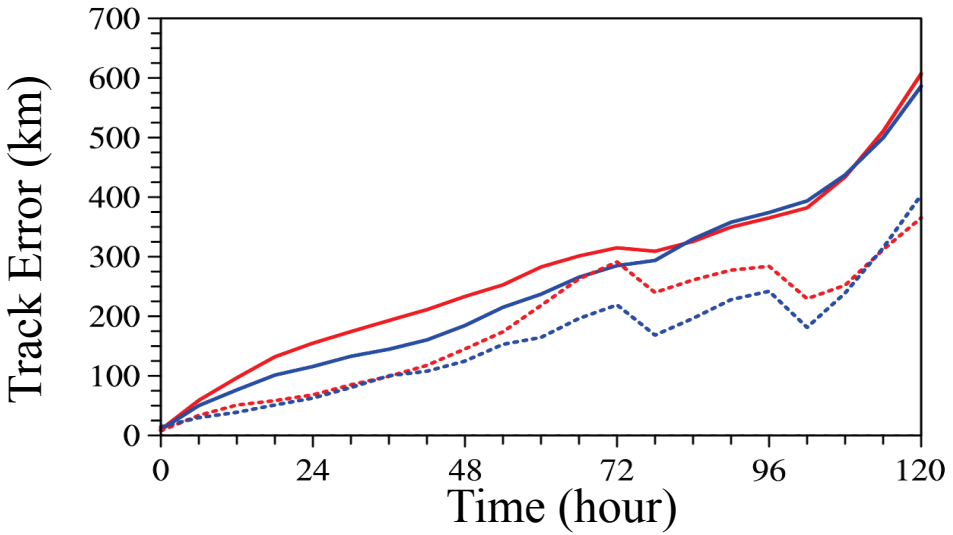

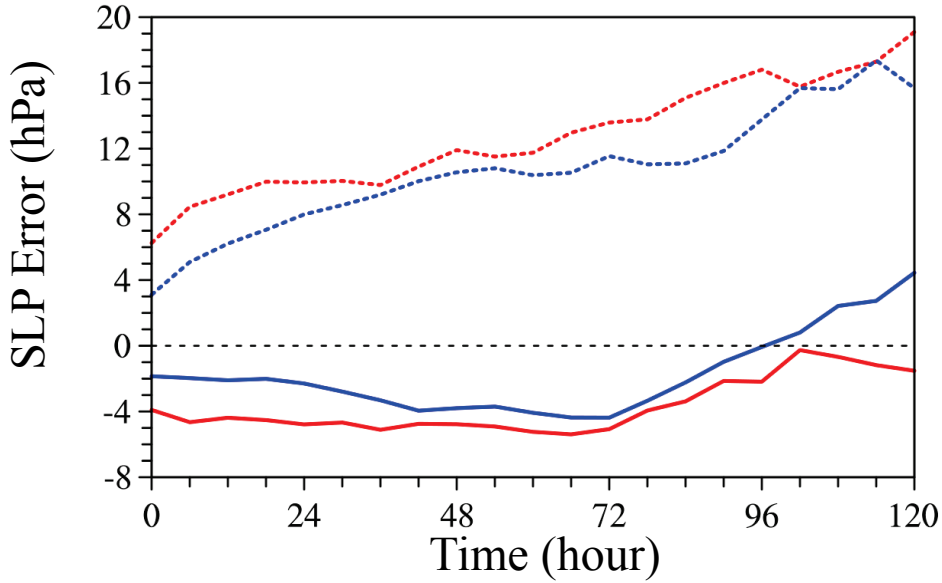

mean L43

mean L61

std. L43

std. L61

Impacts of Suomi NPP ATMS Data Assimilation for TC Track and Intensity Forecasts

The outer domain, ghost domain, middle nest and inner nest of HWRF

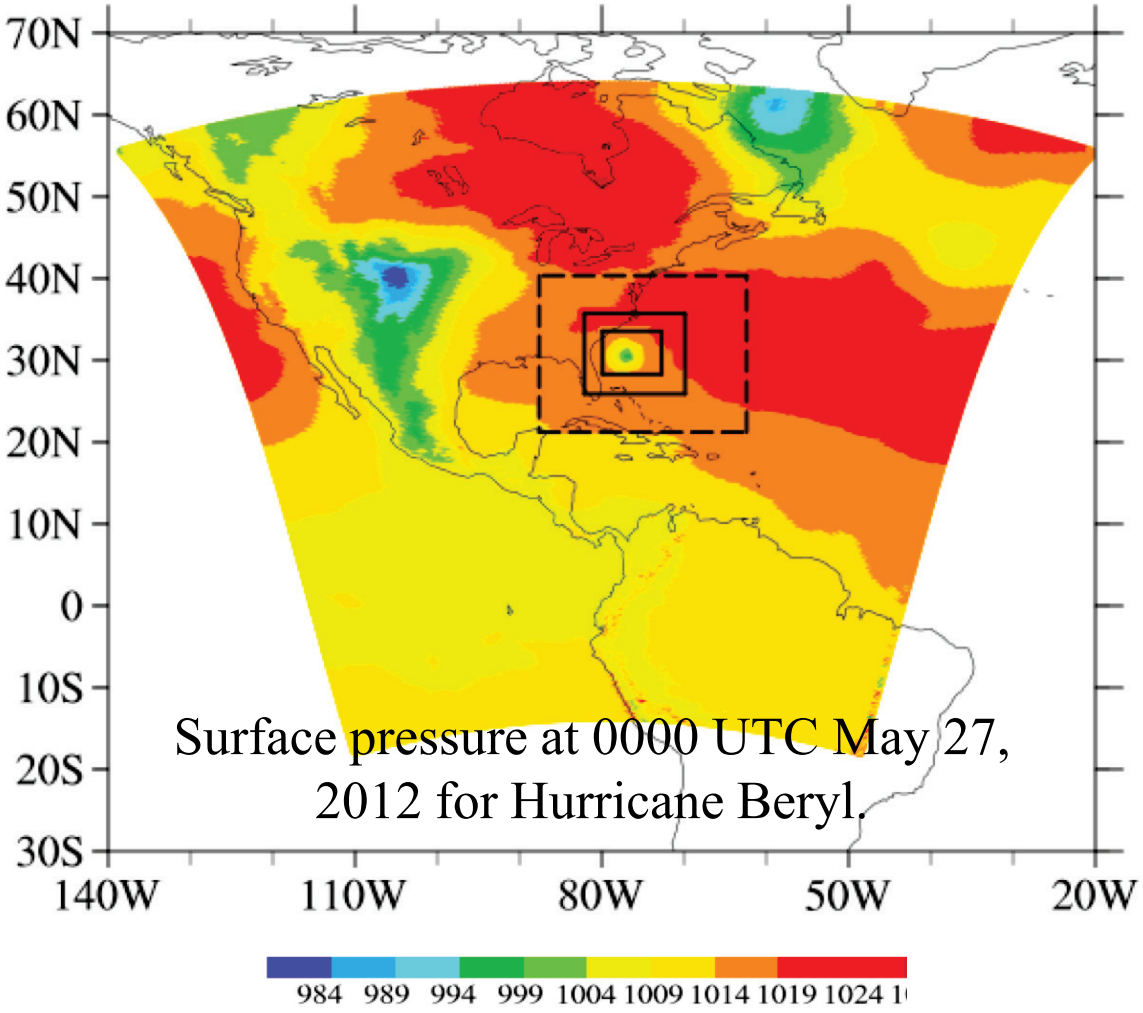

Surface pressure at 0000 UTC May 27, 2012 for Hurricane Beryl.

Cloud and Water Vapor Related QC Parameters

$$LWP = a_0 \cos\theta\left(\ln(T_s - T_{b,2}) - a_1 \ln(T_s - T_{b,1}) - a_2\right)$$ (Weng et al., 2003)

$$IWP^{o,m}_{index} = \mu(c_1 - \mu(c_2 - \mu c_3) + c_4 \times \log(285 - T^{o,m}_{b,1}) - c_5 \times \log(285 - T^{o,m}_{b,2})$$

$$TPW^{o,m}_{index} = \mu(t_1 - \mu(t_2 - \mu t_3) - t_4 \times \log(285 - T^{o,m}_{b,1}) + t_5 \times \log(285 - T^{o,m}_{b,2})$$

$$CLW_{index} = \begin{cases} -0.754 \times \dfrac{T^{o}_{b,1} - T^{m}_{b,1} - \alpha_1}{285 - T^{m}_{b,1}} + 2.265 \times \dfrac{T^{o}_{b,2} - T^{m}_{b,2} - \alpha_2}{285 - T^{m}_{b,2}} & \text{if } T^{m}_{s} > 273.15K \\ 0 & \text{otherwise} \end{cases}$$

$\mu = \cos\theta$, θ is satellite zenith angle

α_i is the scan angle dependent bias of the i^{th} channel

$c_i = 8.24, 2.622, 1.846, 0.754, 2.265$, $t_i = 247.92, 69.235, 44.177, 11.627, 73.409$

O-B Values for Those Data Points that Pass QC

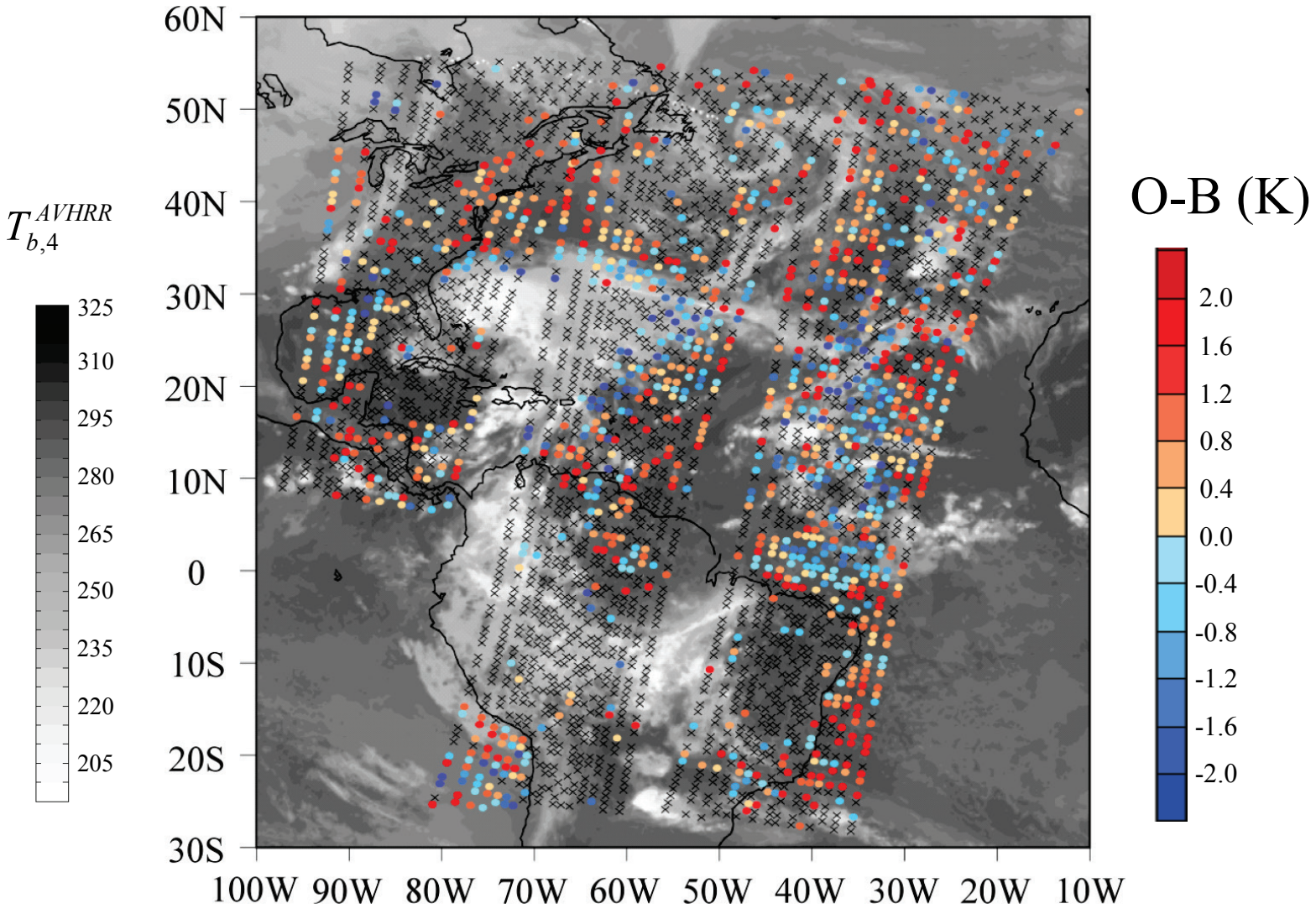

0600 UTC October 26, 2012

Outliers Removed by QC

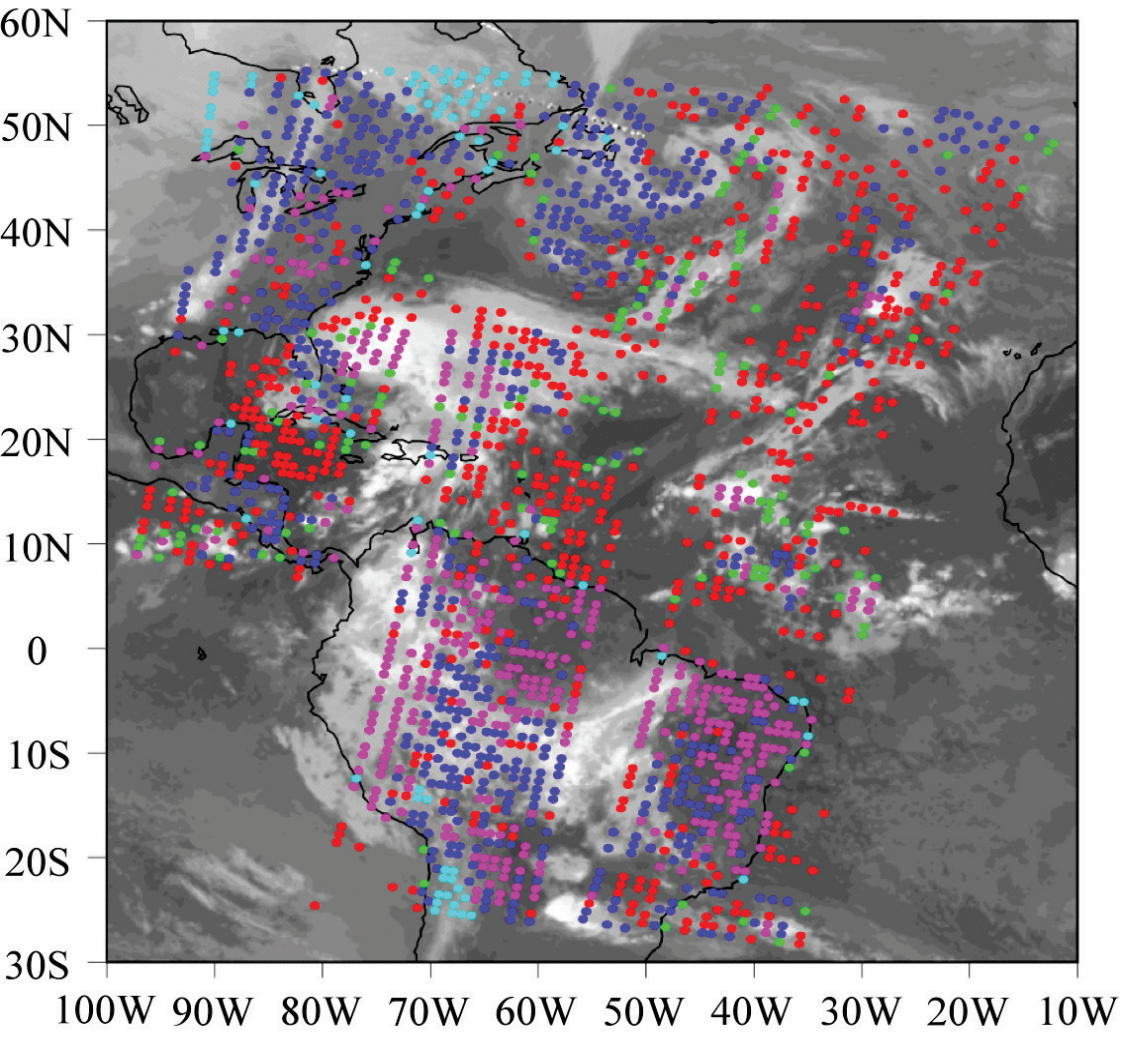

0600 UTC October 26, 2012

- $(O-B)_{ch7}$ is large
- $(O-B)_{ch5}$ and LWP are large
- $(O-B)_{ch}$ > observation error
- $(O-B)_{ch1-3}$ /ε_{ch1-3} are large (ε_{ch1-3} is surface emissivity)
- Mixed surface (a single surface type covers less than 99% of the FOV area

when the sum of the cloud liquid water mixing ratio and cloud ice mixing ratio from the background field is zero.

O-B and O-A Data Counts for Hurricane Isaac

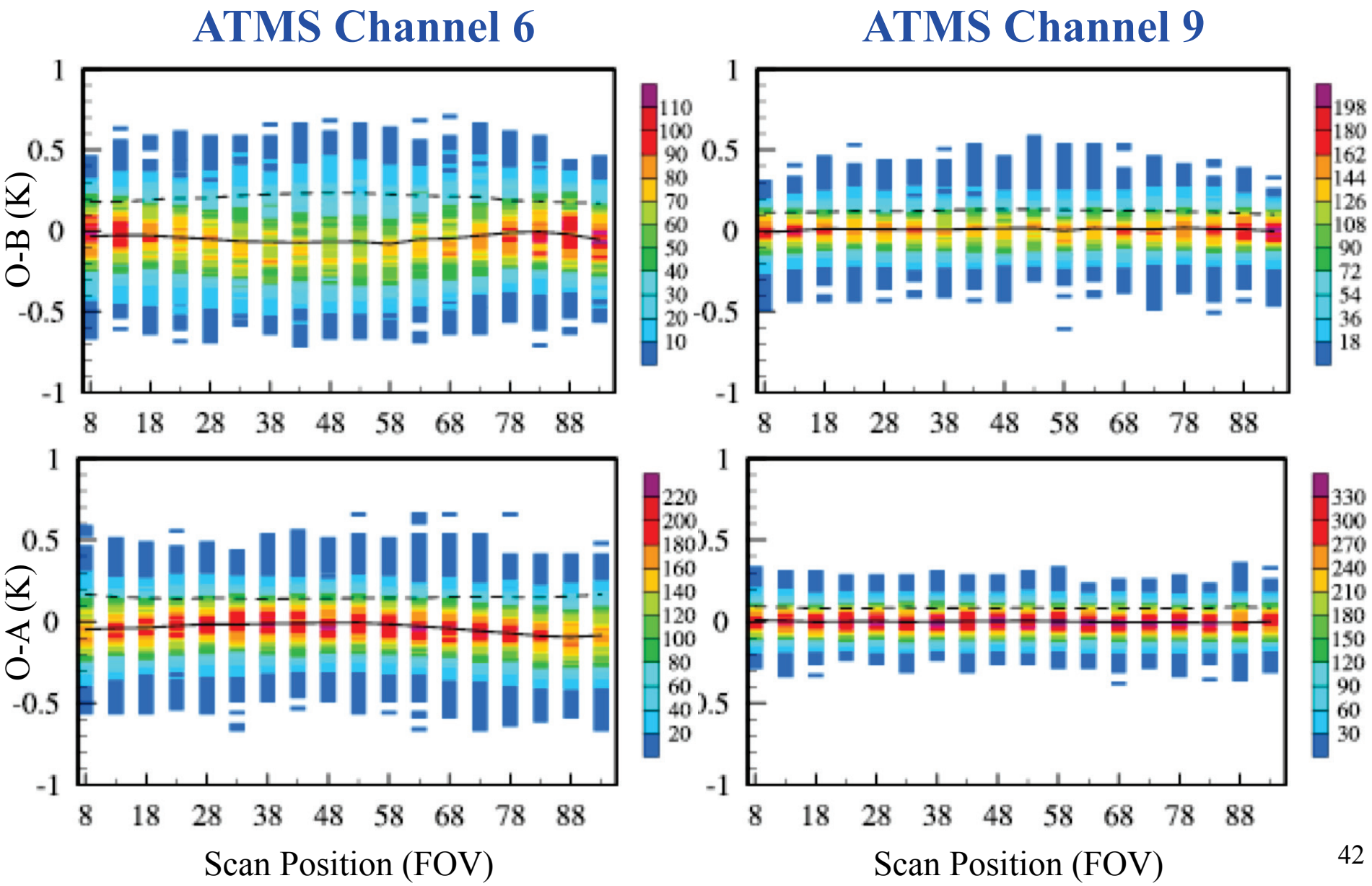

Standard Deviations of O-B and O-A for Hurricane Isaac

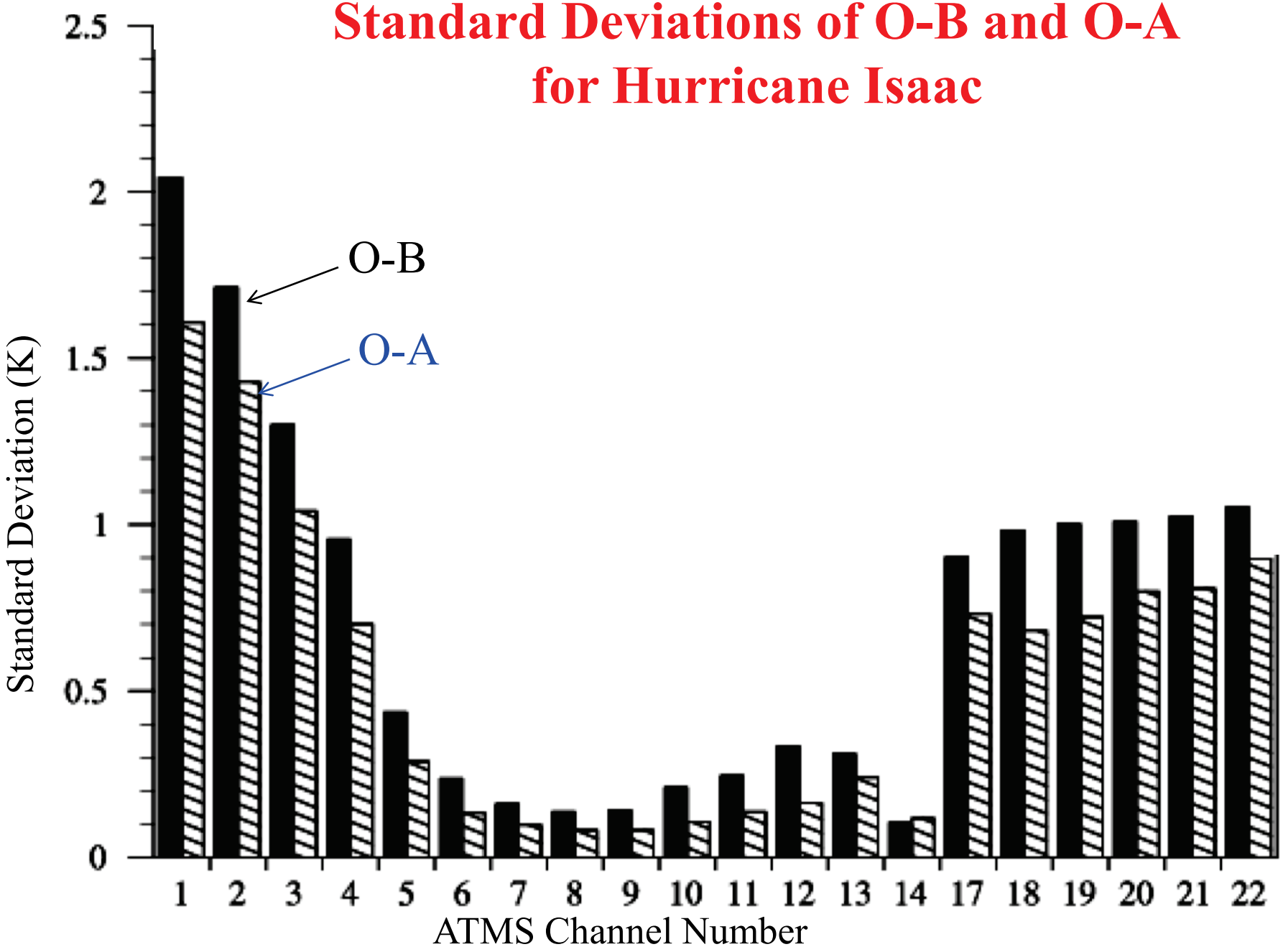

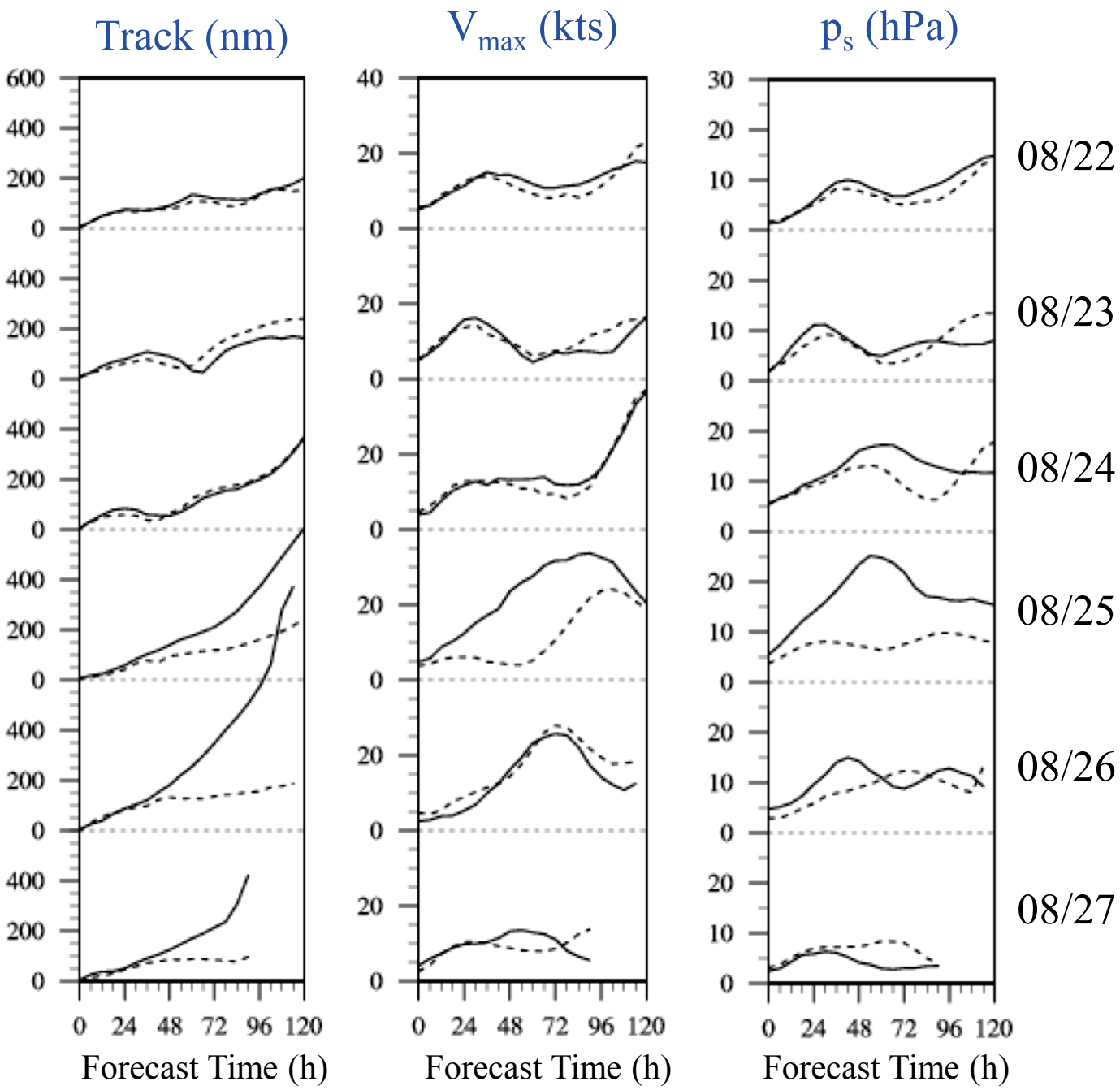

Daily Mean Forecast Errors For Isaac

Impacts on Intensity Forecast Hurricane Isaac

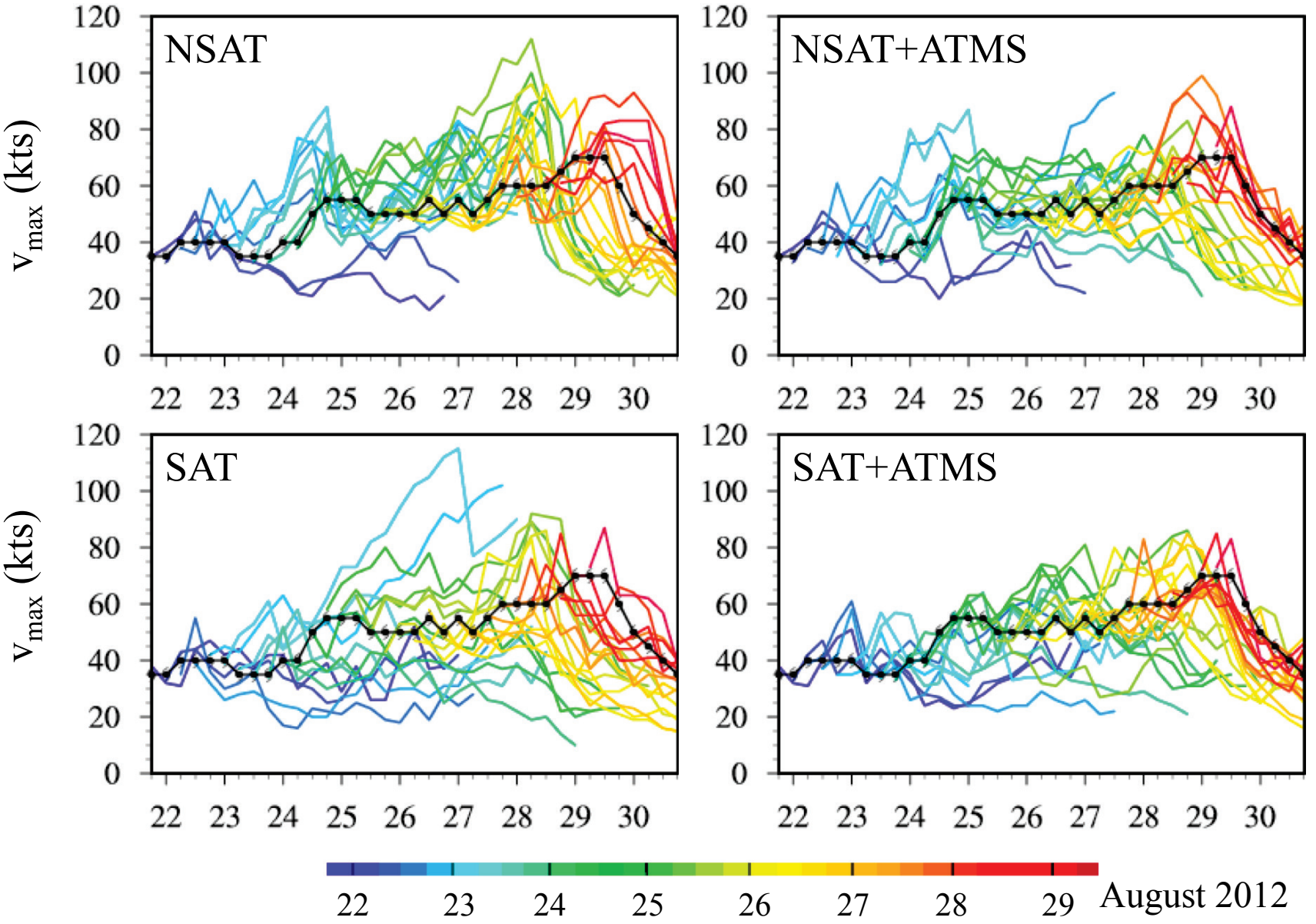

Impacts of ATMS Data Assimilation on Track Forecast of Hurricane Sandy

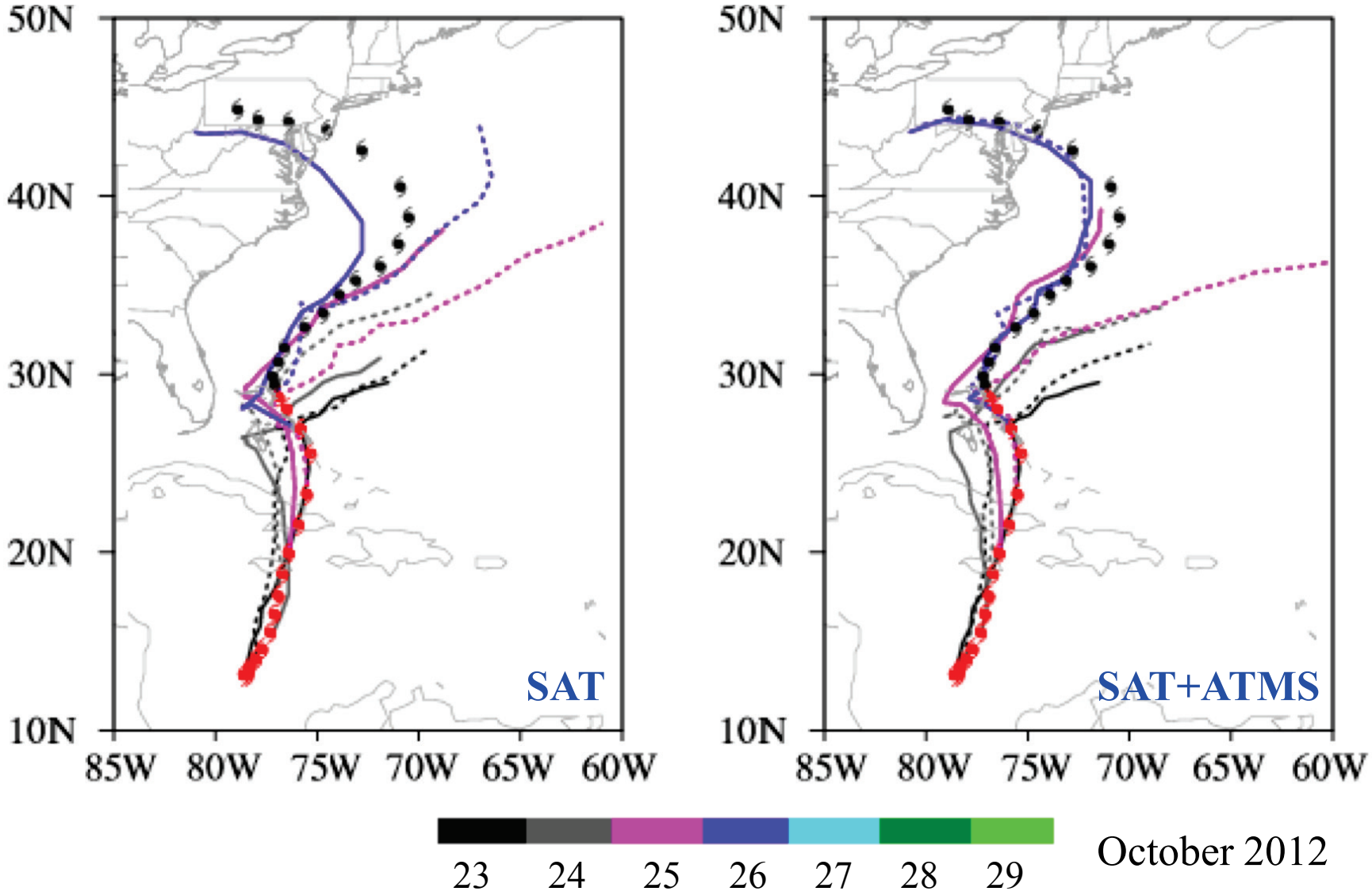

Hurricane Sandy (PV at 200 hPa)

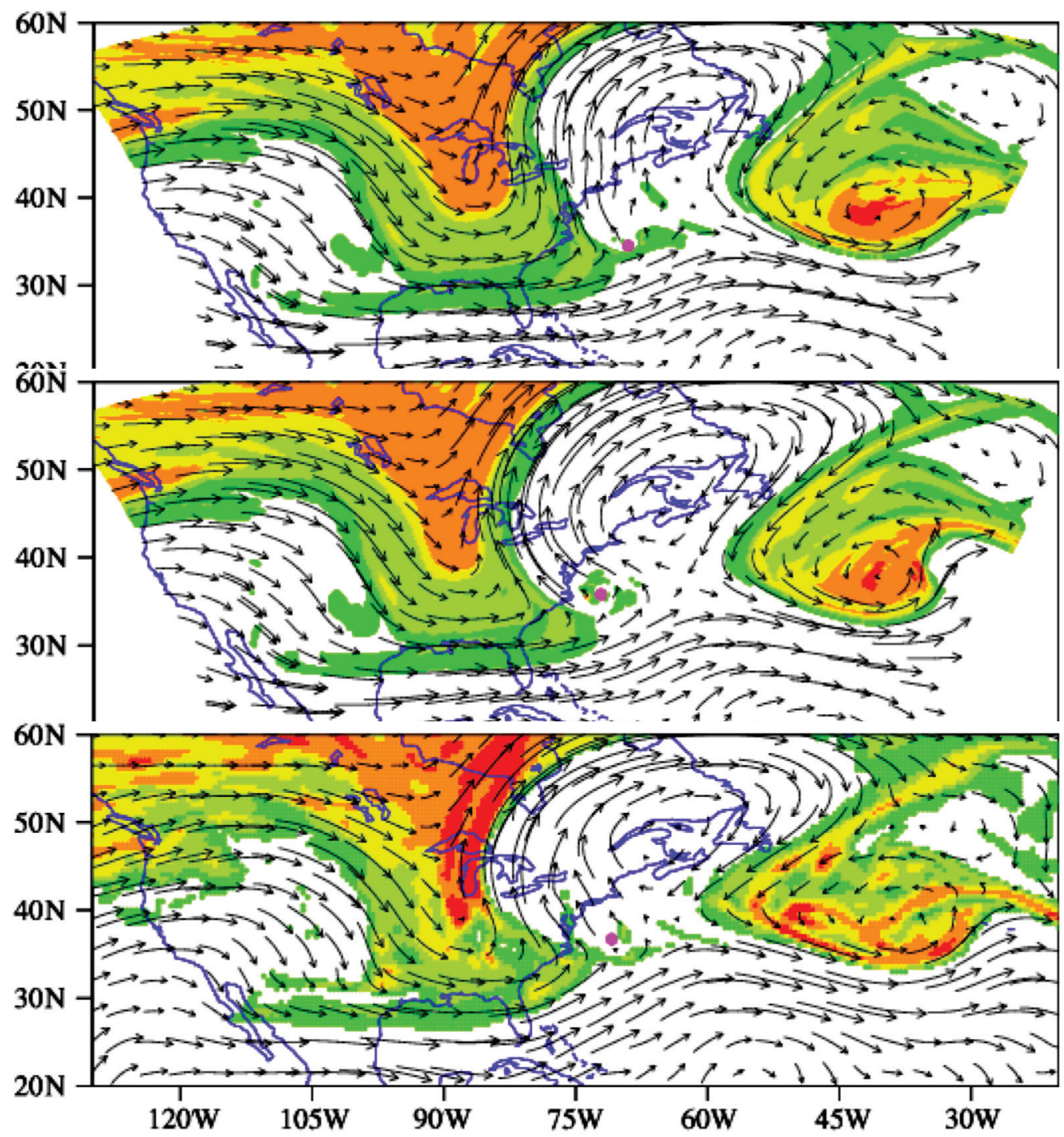

72-h Forecast without ATMS

72-h Forecast with ATMS

NCEP GFS analysis 1200 UTC October 29

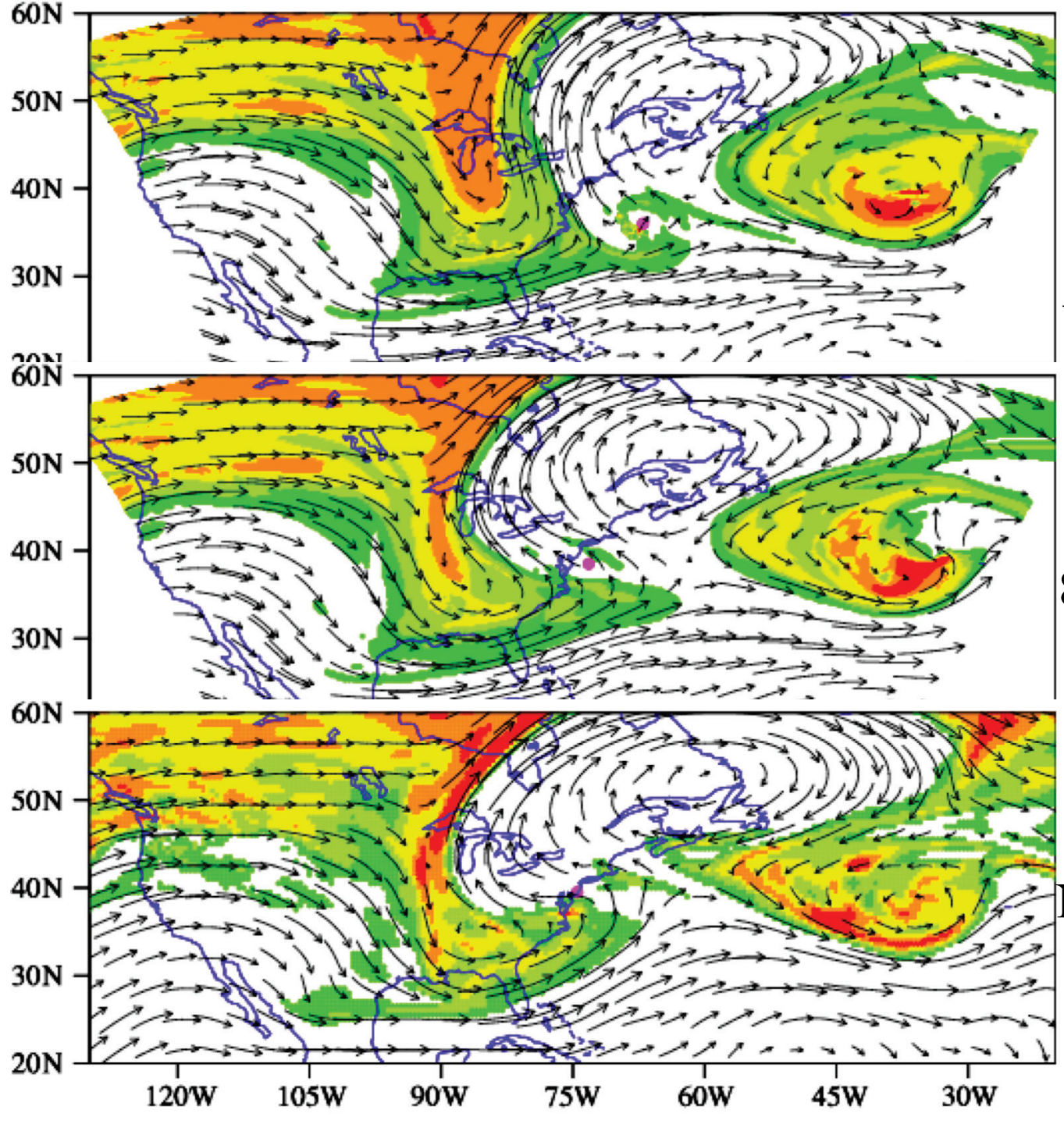

Hurricane Sandy (PV at 200 hPa)

84-h Forecast without ATMS

84-h Forecast with ATMS

NCEP GFS analysis

0000 UTC October 30

84-h Forecasts of Cloud Liquid Water Valid at 0000 UTC 30 October 2012

Without ATMS

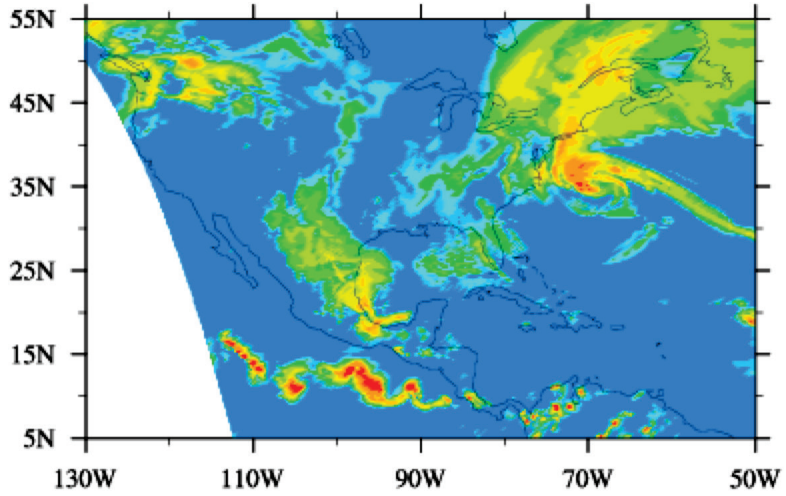

With ATMS

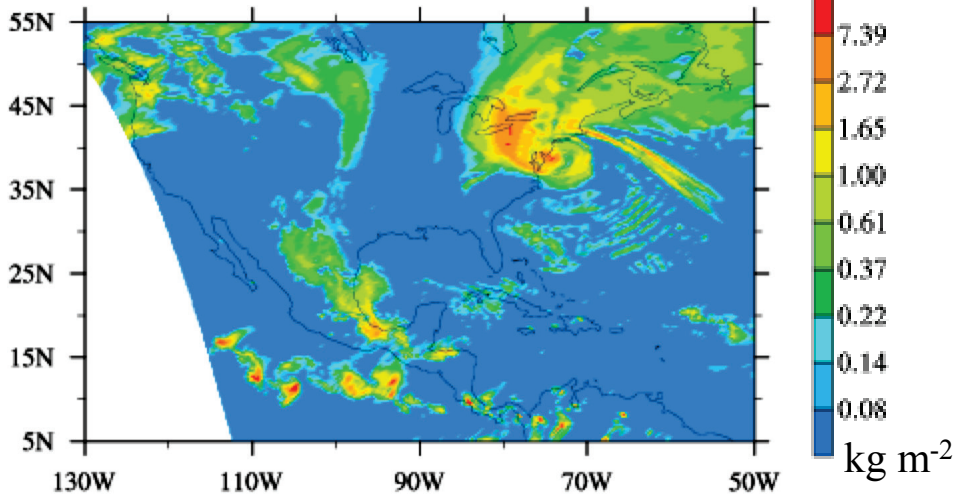

GOES-13 $T_{b,4}$ for Verification

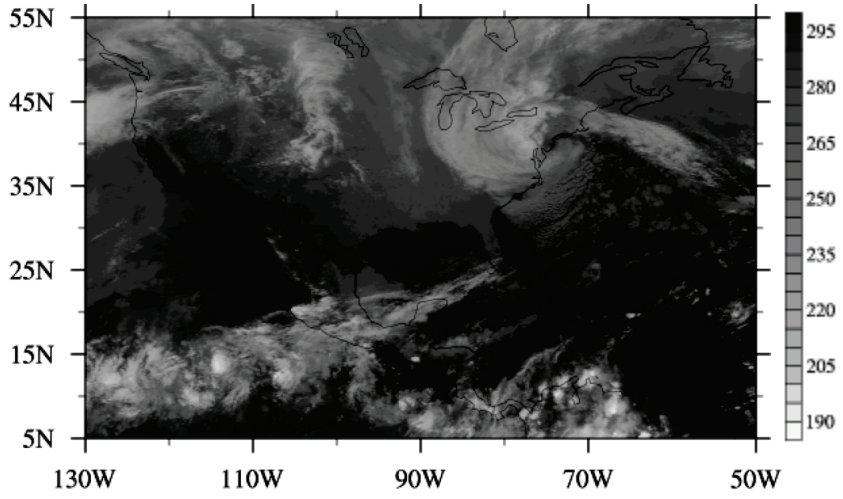

ATMS $T_{b,18}$ at 1727 UTC 10/29/12

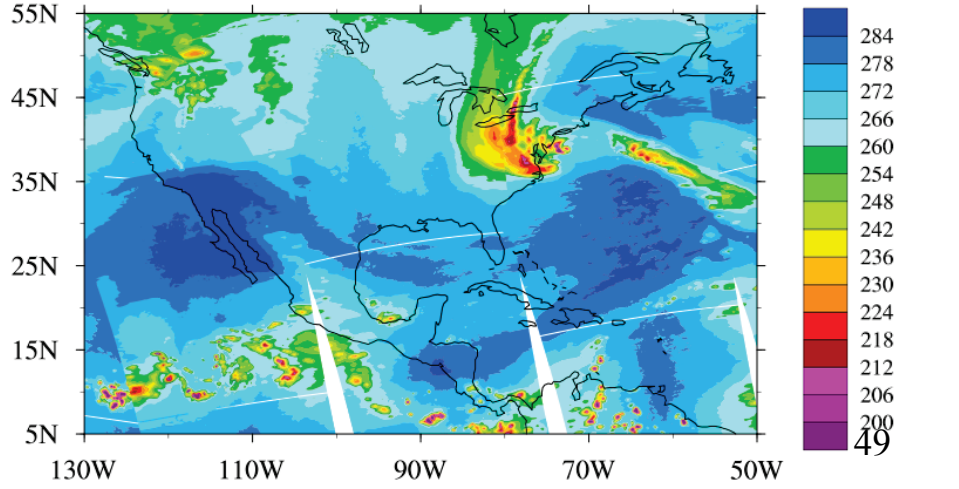

Mean Forecast Errors for Four 2012 Atlantic Hurricanes

Impact of ATMS Data Assimilation

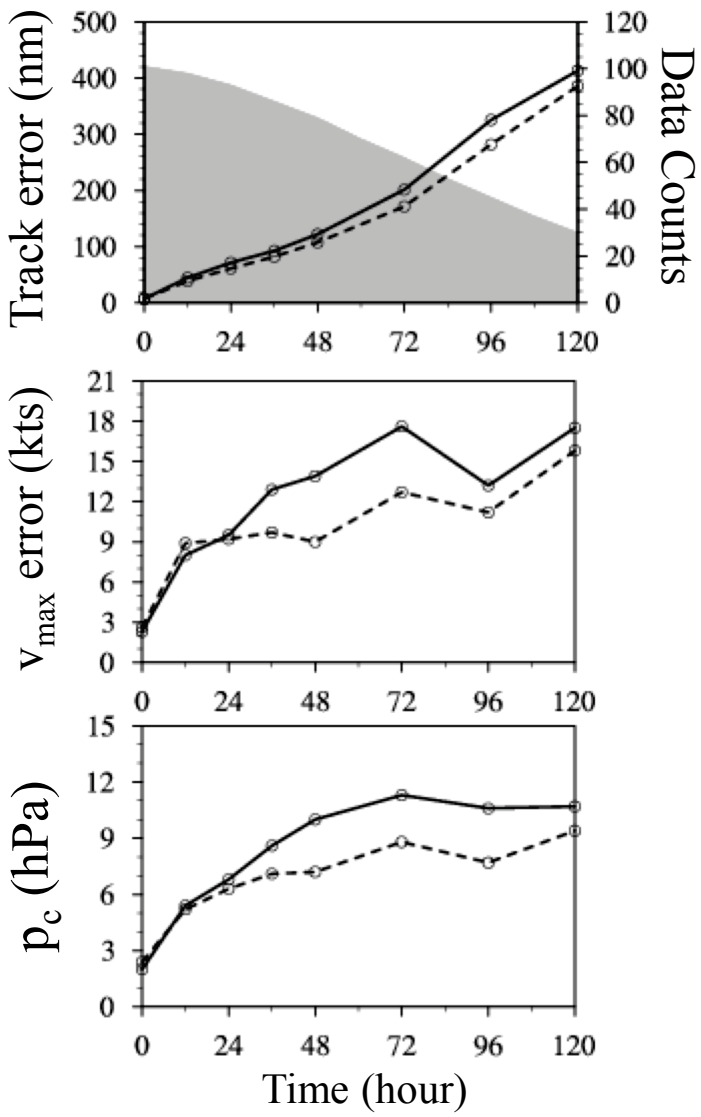

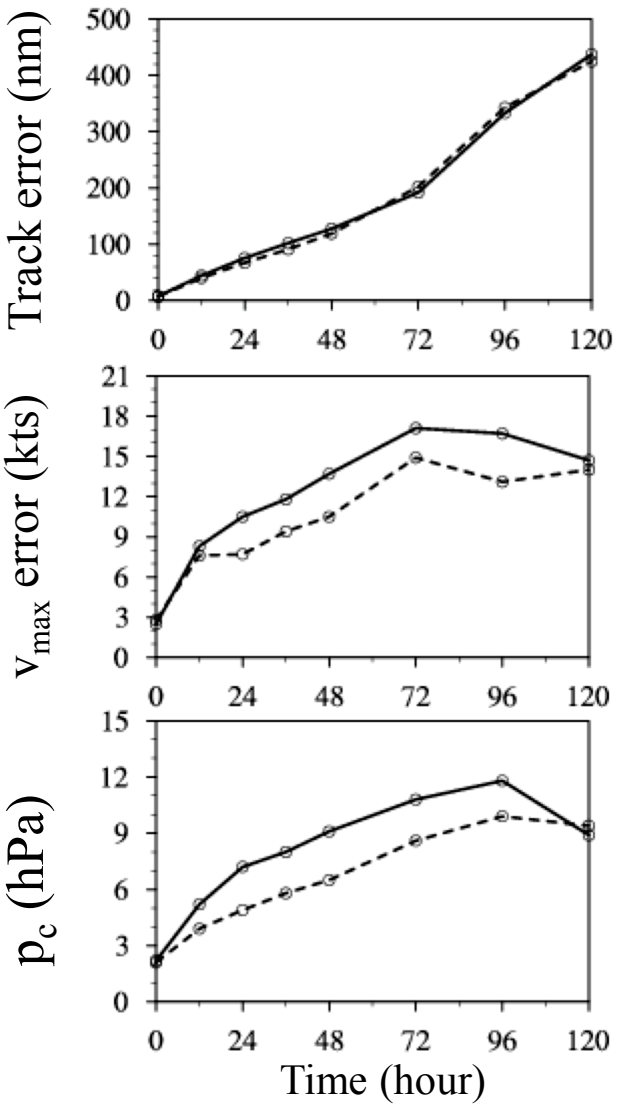

Summary and Conclusions

- A consistent FOV distribution between temperature and humidity channels on ATMS makes the cloud detection easy to implement
- A higher model top allows more upper-level microwave and infrared channels to be assimilated into HWRF, resulting improved atmospheric steering and track forecasts
- ATMS data assimilation in GSI/HWRF results in a consistent positive impact on the track and intensity forecasts of the four landfall hurricanes in 2012
- Hurricane Sandy's forecasts are significantly improved after ATMS data assimilation when verified with independent GOES and POES observations

More details can be found in

Zou, X., F. Weng, Q. Shi, B. Zhang, C. Wu and Z. Qin, 2013a: Satellite data assimilation in NWP models. Part III: Impacts of model top on radiance assimilation in HWRF. *J. Atmos. Sci.*, (submitted)

Zou, X., F. Weng, B. Zhang, L. Lin, Z. Qin and V. Tallapragada, 2013b: Impact of ATMS radiance data assimilation on hurricane track and intensity forecasts using HWRF. *J. Geophys. Res.*, **118**, 11,558-11,576.

Zou, X., Z. Qin and F. Weng, 2013c: Two separate quality control approaches for MHS data assimilation over land and ocean. *J. Atmos. Sci.* (to be submitted)

Weng, F., X. Zou, X. Wang, S. Yang, and M. D. Goldberg, 2012: Introduction to Suomi NPP ATMS for NWP and tropical cyclone applications. *J. Geophy. Res.*, **117**, D19112, 14pp, doi:10.1029/2012JD018144.

Current and Future Plan

- ATMS radiance assimilation (further refinement)
- Model top&vertical levels (further refinement)
- GOES imager radiance assimilation for TCs (on going)
- AMSU three orbits impact assessment (on going)
- CrIS/VIIRS radiance assimilation (on going)
- SSMIS/AMSR2 imager radiance assimilation (on going)
- Combined AMSU-A/MHS data stream (on going)
- Hurricane initialization using satellite data (on going)

Three Key Components for Satellite Data Assimilation

Bias Correction, Data Thinning, Quality Control

Acknowledgement

This work was jointly supported by NSF, NOAA GOES-R risk reduction program and JPSS Proving Ground Program.